CHAPTER

1

Early Replicons: Origin and Evolution*

Peter Schuster and Peter F. Stadler

ABSTRACT

RNA and protein molecules have been found to be both templates for replication and specific catalysts for biochemical reactions. RNA molecules, although very difficult to obtain via plausible synthetic pathways under prebiotic conditions, are the only candidates for early replicons. Only they are obligatory templates for replication, which can conserve mutations and propagate them to forthcoming generations. RNA-based catalysts, called ribozymes, act with high efficiency and specificity for all classes of reactions involved in the interconversion of RNA molecules such as cleavage and template-assisted ligation. The idea of an RNA world was conceived for a plausible prebiotic scenario of RNA molecules operating upon each other and constituting thereby a functional molecular organization. A theoretical account of molecular replication making precise the conditions under which one observes parabolic, exponential, or hyperbolic growth is presented. Exponential growth is observed in a protein-assisted RNA world where plus–minus (±) duplex formation is avoided by the action of an RNA replicase. Error propagation to forthcoming generations is analyzed in the absence of selective by neutral mutants as well as for predefined degrees of neutrality. The concept of an error threshold for sufficiently precise replication and survival of populations derived from the theory of molecular quasispecies is discussed. Computer simulations are used to model the interplay between adaptive evolution and random drift. A model of evolution is proposed that allows for explicit handling of phenotypes.

WHAT IS A REPLICON?

Biology, and evolution in particular, are based on reproduction or multiplication and on variation. Reproduction pure has the property of self-enhancement and leads to exponential growth. Self-enhancement in chemical reactions under isothermal conditions is tantamount to autocatalysis that, in its simplest form, corresponds to a reaction mechanism of the kind:

$$A + Y \xrightarrow{k} 2Y, \qquad (1)$$

*Dedicated to Manfred Eigen, the pioneer of molecular evolution and intellectual father of quasispecies theory, on the occasion of his 80th birthday.

Origin and Evolution of Viruses
ISBN 978-0-12-374153-0

where **A** is the substrate and **Y** the autocatalyst. Being just an autocatalyst is certainly not enough for playing a role at the origin of life or in evolution. An additional *conditio sine qua non* is the property to act as an encoded instruction for the reproduction process. It is useful to remain rather vague as far as the nature of this instruction is concerned, because there are many possible solutions for template action at the molecular level. In reality the most straightforward candidates for useful templates are heteropolymers built from a few classes of monomers with specific interactions. The proper physical basis for such interactions are charge patterns, patterns of hydrogen bonds, space-filling hydrophobic interactions, and others. We may summarize the first paragraph by saying: "A replicon is an entity that carries the instruction for its own replication in some encoded form."

Precise asexual reproduction gives rise to perfect inheritance. This is essentially true for prokaryotes: bacteria, archaebacteria, and viruses. In sexually reproducing eukaryotes, recombination introduces variation already into the error-free reproduction process.[1] Mutation in the form of unprecise or error-prone reproduction represents the universal kind of variation, which occurs in all organisms and can be sketched by a single overall reaction step:

$$\mathrm{A} + \mathrm{Y} \xrightarrow{k'} \mathrm{Y} + \mathrm{Y}'. \qquad (2)$$

Here, the mutant is denoted by $\mathbf{Y}'$. The rate parameters k and k' refer to two parallel reaction channels. This can be indicated by replacing the two parameters with a single rate constant and reaction (channel) frequencies:

$$\begin{aligned} k &\Rightarrow f \cdot Q \text{ and} \\ k' &\Rightarrow f \cdot Q'. \end{aligned} \qquad (3)$$

[1] Sexual reproduction introduces obligatory recombination into the mechanism of inheritance. Recombination in eukaryotes occurs during meiosis and is a highly complex process. In this chapter we are discussing primitive replication systems only and therefore we can dispense with any detailed discussion of recombination.

In the (improbable) case that $\mathbf{Y}'$ is the only mutant of **Y**, the two channel frequencies add up to unity: $Q + Q' = 1$. In general, there will be many mutations, $\mathbf{Y}_j \rightarrow \mathbf{Y}_i$, that give rise to variants and conservation of probabilities then leads to the conservation relation:

$$\sum_{i=1}^{n} Q_{ij} = 1 \;\forall\; j = 1, \ldots n, \qquad (4)$$

which expresses that a copy is either error free or contains errors.

It is useful further to distinguish two classes of replicons: (i) obligatory replicons and (ii) optional replicons. All error copies of obligatory replicons can be replicated and thus are replicons themselves. Examples of obligatory replicons are nucleic acid molecules under suitable conditions (Figure 1.1). In Nature practically no restrictions on the initiation and chain propagation of replication are known apart from recognition sites at replication origins and a few other general requirements for replication. An example of a laboratory system is the polymerase chain reaction (PCR), which allows for amplification of DNA templates with (almost) any sequence. Optional replicons are, for example, autocatalytically growing oligonucleotides (von Kiedrowski, 1986) and oligopeptides (Lee *et al.*, 1996) (Figure 1.2). These oligomers lose their capability to act as template (almost always) when a particular nucleotide or amino acid residue is exchanged for any other one. In other words, the property to be a replicon is not common feature of the entire class of molecules but a specific property of certain selected molecules only.

Simple replicons certainly lack the complexity of present-day organisms and are defined best as molecular entities that are capable of replication by means of some mechanism based on interaction with a template. Almost all known replicons are oligomers or polymers composed from a few classes of monomers. Two extreme types of replicons are distinguished: *obligatory replicons*, for which exchange of individual monomeric units yields other replicons with different monomer sequences, and

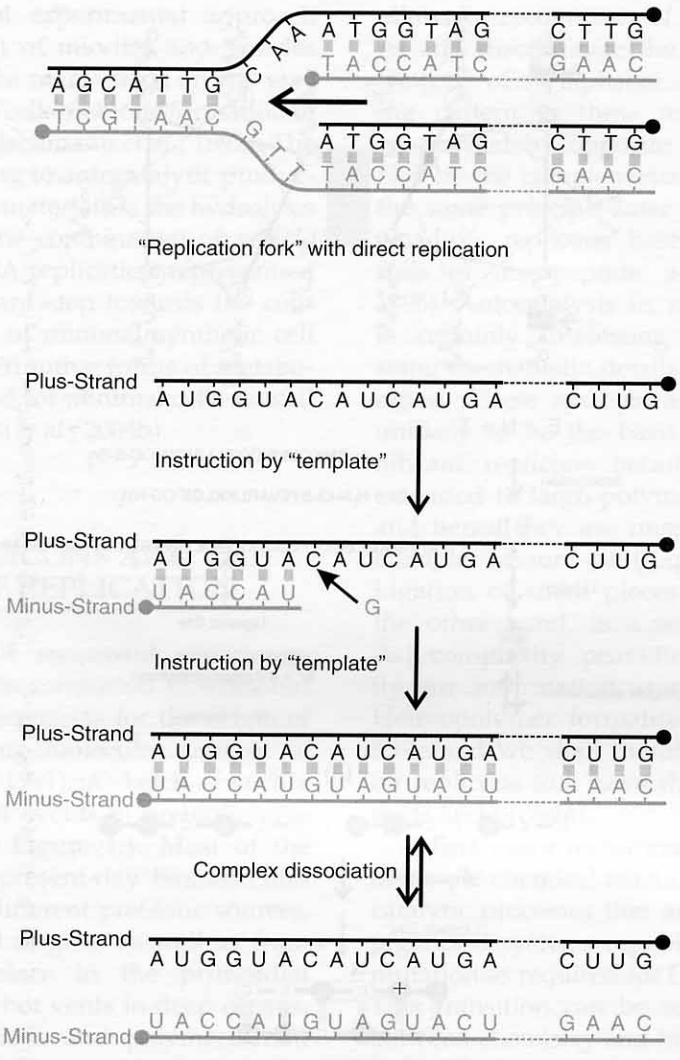

FIGURE 1.1 Template-induced replication of nucleic acids molecules. Direct replication (upper part) is primarily occurring with DNA. It represents a highly sophisticated process involving some 20 enzymes. Template-induced DNA synthesis occurs at the "replication fork," both daughter molecules carry one DNA strand of the parent molecule. Complementary replication (lower part) occurs in Nature with single-stranded RNA molecules. The problem in uncatalyzed complementary replication is complex dissociation. A single enzyme is sufficient for complementary replication of simple RNA bacteriophages, since it causes the separation of plus and minus strands during replication. The two strands separate and form their own single-strand structures before the double helix is completed. Polymerase chain reaction (PCR) follows essentially the same mechanism of complementary replication as shown here. The separation of the two strands of the double helix is accomplished by heating: the complex dissociates spontaneously at higher temperature.

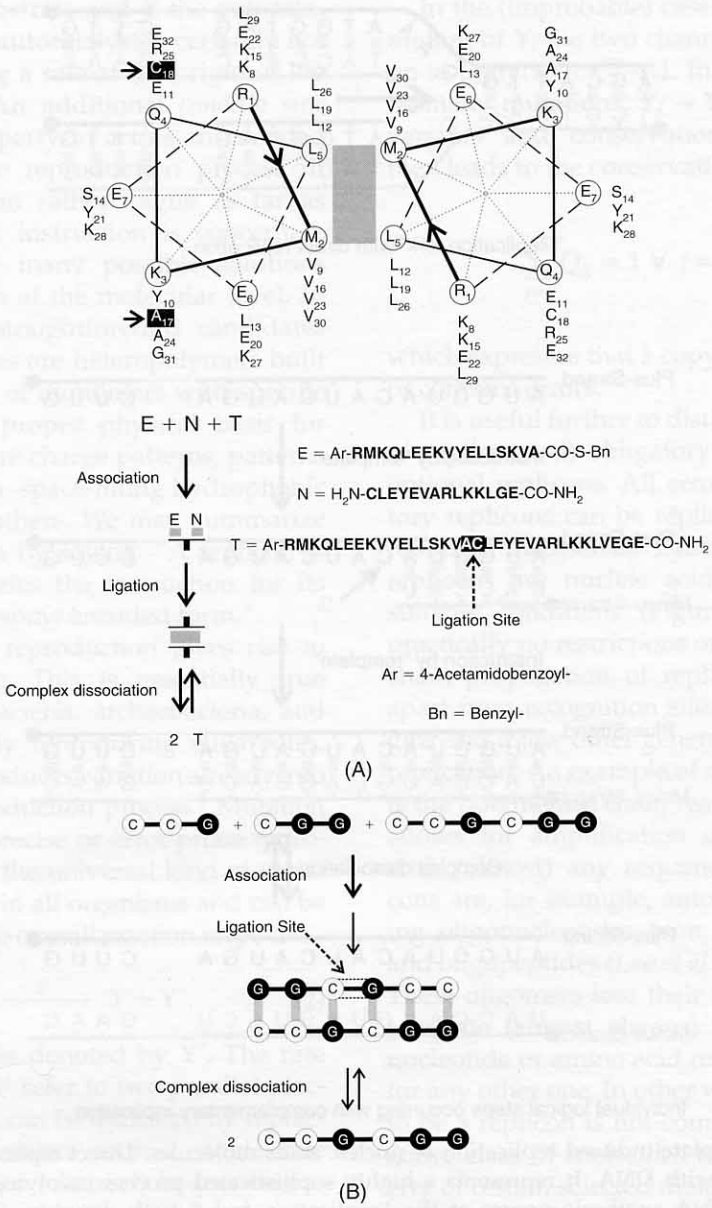

FIGURE 1.2 Oligopeptide and oligonucleotide replicons. (A) An autocatalytic oligopeptide that makes use of the leucine zipper for template action. The upper part illustrates the stereochemistry of oligopeptide template–substrate interaction by means of the helix wheel. The ligation site is indicated by arrows. The lower part shows the mechanism (Lee *et al.*, 1996; Severin *et al.*, 1997). (B) Template-induced self-replication of oligonucleotides (von Kiedrowski (1986)) follows essentially the same reaction mechanism. The critical step is the dissociation of the dimer after bond formation which commonly prevents these systems from exponential growth and Darwinian behavior.

optional replicons where the capability of replication is restricted to certain specific sequences.

More complex replicons (not discussed in detail here) including DNA and protein, compartment structure, and metabolism have been considered as well (Eigen and Schuster, 1982; Gánti, 1997; Szathmáry and Maynard Smith, 1997; Rasmussen *et al.*, 2003; Luisi,

2004). A successful experimental approach to self-reproduction of micelles and vesicles highlights one of the many steps on the way towards a primitive cell: prebiotic formation of vesicle structures (Bachmann *et al.*, 1992). The basic reaction leading to autocatalytic production of amphiphilic materials is the hydrolysis of ethyl caprate. The combination of vesicle formation with RNA replication represents a particularly important step towards the construction of a kind of minimal synthetic cell (Luisi *et al.*, 1994). Primitive forms of metabolism were considered for minimal cells as well (see, e.g., Rasmussen *et al.*, 2004b).

SIMPLE REPLICONS AND THE ORIGIN OF REPLICATION

A large number of successful experimental studies have been conducted to work out plausible chemical scenarios for the origin of early replicons being molecules capable of replication (Mason, 1991). A sketch of such a possible sequence of events in prebiotic evolution is shown in Figure 1.1. Most of the building blocks of present-day biomolecules are available from different prebiotic sources, from extraterrestrial origins, as well as from processes taking place in the primordial atmosphere or near hot vents in deep oceans. Condensation reactions and polymerization reactions formed non-instructed polymers, for example random oligopeptides of the protenoid type (Fox and Dose, 1977).

Template catalysis opens up the door to molecular copying and self-replication. Several small templates were designed by Rebek and co-workers and these molecules do indeed show complementarity and undergo complementary replication under suitable conditions (see, e.g., Tjivikua *et al.*, 1990; Nowick *et al.*, 1991). Like nucleic acids they consist of a backbone whose role is to bring "molecular digits" into stereochemically appropriate positions, so that they can be read by their complements. Complementarity is also based on essentially the same principle as in nucleic acids: Specific patterns of hydrogen bonds allow for recognition of complementary digits and discriminate the non-complementary "letters" of an alphabet. The hydrogen bonding pattern in these model replicons may be assisted by opposite electric charges carried by the complements. We shall encounter the same principle later in the discussion of Ghadiri's replicons based on stable coiled-coils of oligopeptide α-helices (Lee *et al.*, 1996). Autocatalysis in small model systems is certainly interesting because it reveals some mechanistic details of molecular recognition. These systems are, however, highly unlikely to be the basis of biologically significant replicons because they cannot be extended to large polymers in a simple way and hence they are unsuitable for storing a sizeable amount of (sequence) information. Ligation of small pieces to larger units, on the other hand, is a source of combinatorial complexity providing sufficient capacity for information storage and evolution. Heteropolymer formation thus seems inevitable and we shall therefore focus here only on replicons that have this property: nucleic acids and proteins.

A first major transition leads from a world of simple chemical reaction networks to autocatalytic processes that are able to form self-organized systems capable of replication and mutation as required for Darwinian evolution. This transition can be seen as the interface between chemistry and biology since an early Darwinian scenario is tantamount to the onset of biological evolution. Two suggestions were made in this context: (i) autocatalysis arose in a network of reactions catalyzed by oligopeptides (Kauffman, 1993) and (ii) the first autocatalyst was a representative of a class of molecules with obligatory template function in the sense discussed above (Eigen, 1971; Orgel, 1987). The first suggestion works with molecules that are easily available under prebiotic conditions but lacks plausibility because the desired properties—conservation and propagation of mutants—are unlikely to occur with oligopeptides. The second concept suffers from the opposite: it is very hard to derive a plausible scenario for the appearance of the first nucleic acid-like molecules. Once formed,

however, they would fulfill most functional requirements for evolutionary optimization.

Until the 1980s biochemists had an empirically well established but nevertheless prejudiced view on the natural and artificial functions of proteins and nucleic acids. Proteins were thought to be Nature's unbeatable universal catalysts, highly efficient as well as ultimately specific, and as in the case of immunoglobulins even tunable to recognize previously unseen molecules. After Watson and Crick's famous discovery of the double helix, DNA was considered to be the molecule of inheritance, capable of encoding genetic information and sufficiently stable to allow for essential conservation of nucleotide sequences over many replication rounds. RNA's role in the molecular concert of Nature was reduced to the transfer of sequence information from DNA to protein, either as mRNA or as tRNA. Ribosomal RNA and some rare RNA molecules did not fit well into this picture: Some sort of scaffolding functions were attributed to them, such as holding supramolecular complexes together or bringing protein molecules into the correct spatial positions required for their functions.

This conventional picture was based on the idea of a complete "division of labor." Nucleic acids, DNA, as well as RNA were the templates, ready for replication and read-out of genetic information but not to do catalysis. Proteins were the catalysts and thus not capable of template function. In both cases these rather dogmatic views turned out to be wrong. In the 1980s Cech and Altman discovered RNA molecules with catalytic functions (Cech, 1983, 1986, 1990; Guerrier-Takada *et al.*, 1983). The name "ribozyme" was created for this new class of biocatalysts because they combine the properties of ribonucleotides and enzymes. Their examples dealt with RNA cleavage reactions catalyzed by RNA; without the help of a protein catalyst a non-coding region of an RNA transcript, a group I intron, cuts itself out during mRNA maturation. The second example concerns the enzymatic reaction of RNaseP, which catalyzes tRNA formation from the precursor poly-tRNA. For a long time biochemists had known that this enzyme consists of a protein and an RNA moiety. It was tacitly assumed that the protein was the catalyst while the RNA component had only a backbone function. The converse, however, is true: the RNA acts as catalyst and the protein provides merely a scaffold required to enhance the efficiency. Even more spectacular was the result from the structure of the ribosome at atomic resolution (Ban *et al.*, 2000; Nissen *et al.*, 2000; Steitz and Moore, 2003): polypeptide synthesis at the ribosome is catalyzed by rRNA and not by ribosomal proteins.

The second prejudice was disproved only about ten years ago by the demonstration that oligopeptides can act as templates for their own synthesis and thus show autocatalysis (Lee *et al.*, 1996; Severin *et al.*, 1997; Lee *et al.*, 1997). In this very elegant work, Ghadiri and co-workers have demonstrated that template action does not necessarily require hydrogen bond formation. Two smaller oligopeptides of chain lengths 17 (E) and 15 (N) are aligned on the template (T) by means of the hydrophobic interaction in a coiled-coil of the leucine zipper type and the 32-mer is produced by spontaneous peptide bond formation between the activated carboxygroup and the free amino residue (Figure 1.2A). The hydrophobic cores of template and ligands consist of alternating valine and leucine residues and show a kind of knobs-into-holes type packing in the complex. The ability of proteins to act as templates is a consequence of the three-dimensional structure of the protein α-helix, which allows the formation of coiled-coils. It requires that the residues making the contacts between the helices fulfill the condition of space filling and thus stable packing. Modification of the oligopeptide sequences alters the interaction in the complex and thereby modifies the specificity and efficiency of catalysis.

A highly relevant feature of oligopeptide self-replication concerns the easy formation of higher replication complexes: Coiled-coil formation is not restricted to two interacting helices; triple helices and higher complexes are known to be very stable as well. Autocatalytic oligopeptide formation may thus involve not

only a template and two substrates but, for example, a template and a catalyst that form a triple helix together with the substrates (Severin *et al.*, 1997). Only a very small fraction of all possible peptide sequences fold into three-dimensional structures that are suitable for leucine zipper formation and hence a given autocatalytic oligopeptide is very unlikely to retain the capability of template action on mutation. Peptides are thus optional templates and replicons on a peptide basis are rare.

In contrast to the volume-filling principle of protein packing, the specificity of catalytic RNAs is provided by base pairing and to a lesser extent by tertiary interactions. Both are the results of hydrogen bond specificity. Metal ions, in particular Mg^{2+}, are often involved in RNA structure formation and catalysis, too. The catalytic action of RNA on RNA is exercised in the co-folded complexes of ribozyme and substrate. Since the formation of a catalytic center of a ribozyme that operates on another RNA molecule requires sequence complementarity in parts of the substrate, ribozyme specificity is thus predominantly reflected by the sequence and not by the three-dimensional structure of the isolated substrate. Template action of nucleic acid molecules—being the basis for replication—is a direct consequence of the structure of the double helix. It requires an appropriate backbone provided by the antiparallel ribose-phosphate or 2′-deoxyribose-phosphate chains and a suitable geometry of the complementary purine–pyrimidine pairs. All RNA (and DNA) molecules, however, share these features which, accordingly, are independent of sequence. Every RNA molecule has a uniquely defined complement. Nucleic acid molecules, in contrast to proteins, are therefore obligatory templates. This implies that mutations are conserved and readily propagated into future generations.

Enzyme-free template-induced synthesis of longer RNA molecules from monomers, however, has not been successfully achieved so far (see, e.g., Orgel, 1986). A major problem, among others, is the dissociation of double-stranded molecules at the temperature of efficient replication. If monomers bind with sufficiently high binding constants to the template in order to guarantee the desired accuracy of replication, the new molecules are too sticky to dissociate after the synthesis has been completed. Autocatalytic template-induced synthesis of oligonucleotides from smaller oligonucleotide precursors was nevertheless successful: a hexanucleotide through ligation of two trinucleotide precursors was carried out by von Kiedrowski (1986). His system is the oligonucleotide analogue of the autocatalytic template-induced ligation of oligopeptides discussed above (Figure 1.2). In contrast to the latter system, the oligonucleotides do not form triple-helical complexes. Isothermal autocatalytic template-induced synthesis, however, cannot be used to prepare longer oligonucleotides because of the duplex dissociation problem as mentioned for the template-induced polymerization of monomers.

RNA CATALYSIS AND THE RNA WORLD (FIGURE 1.3)

The first natural ribozymes to be discovered were all RNA-cleaving molecules: the RNA moiety of RNase P (Guerrier-Takada *et al.*, 1983), the class I introns (Cech, 1983), as well as the first small ribozyme called "hammerhead" (Figure 1.4) because of its characteristic secondary structure shape (Uhlenbeck, 1987). Three-dimensional structures are now available for three classes of RNA-cleaving ribozymes (Pley *et al.*, 1994; Scott *et al.*, 1995; Cate *et al.*, 1996; Ferré-D'Amaré *et al.*, 1998) and these data revealed the mechanism of RNA-catalyzed cleavage reactions in full molecular detail. Additional catalytic RNA molecules were obtained through selection from random or partially random RNA libraries and subsequent evolutionary optimization. RNA catalysis in non-natural ribozymes is not only restricted to RNA cleavage: some ribozymes show ligase activity (Bartel and Szostak, 1993; Ekland *et al.*, 1995) and many efforts were undertaken to prepare a ribozyme with full RNA replicase activity. The attempt that comes closest to the

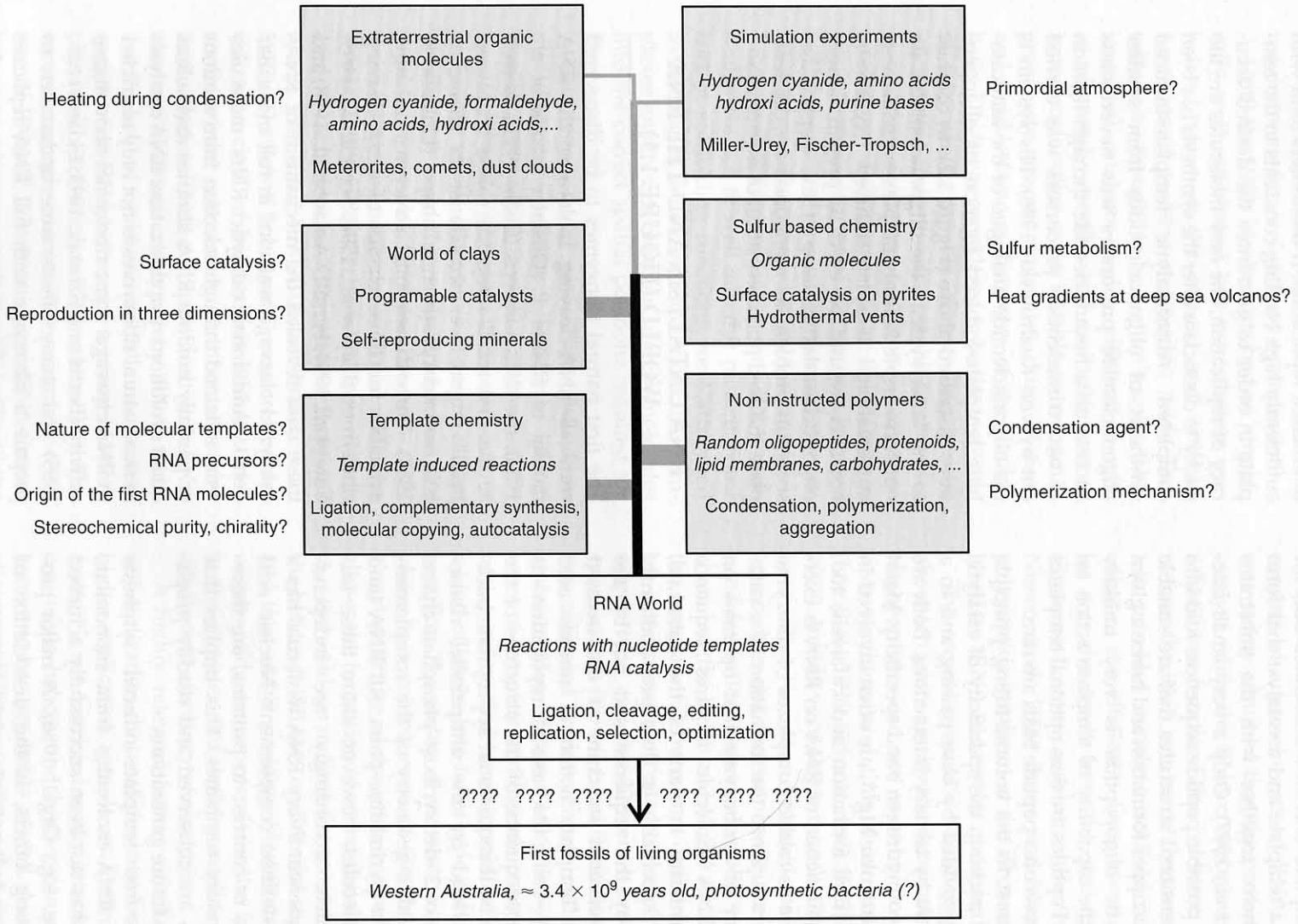

FIGURE 1.3 The RNA world. The concept of a precursor world preceding present-day genetics based on DNA, RNA, and protein is based on the idea that RNA can act as both storage of genetic information and specific catalyst for biochemical reactions. An RNA world is the first scenario on the route to present-day organisms that allows for Darwinian selection and evolution. The question marks along this road to early life indicate important problems. Little is known about further steps (not shown here explicitly) from early replicons to the first cells (Eigen and Schuster, 1982; Maynard Smith and Szathmáry, 1995).

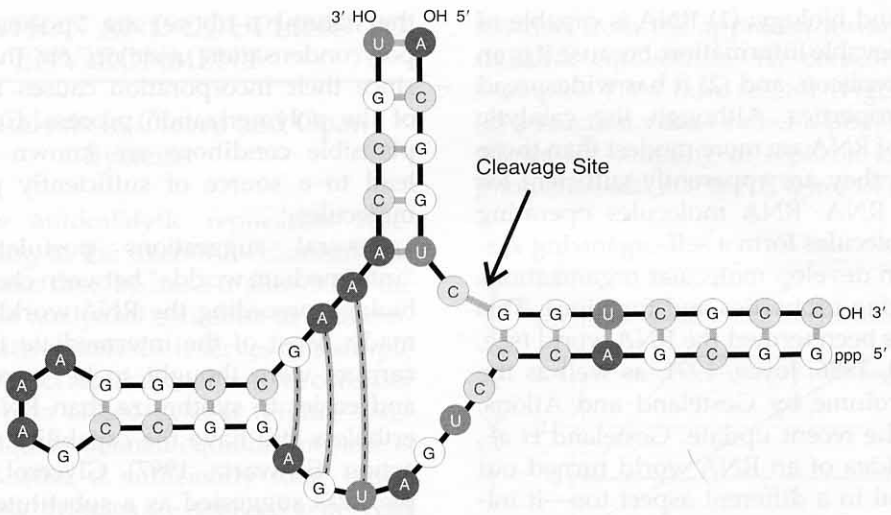

FIGURE 1.4 The hammerhead ribozyme. The substrate is a tridecanucleotide forming two double-helical stacks together with the ribozyme ($n = 34$) in the co-folded complex (Pley *et al.*, 1994). Some tertiary interactions indicated by broken lines in the drawing determine the detailed structure of the hammerhead ribozyme complex and are important for the enzymatic reaction cleaving one of the two linkages between the two stacks. Substrate specificity of ribozyme catalysis is caused by the secondary structure in the co-folded complex between substrate and catalyst.

goal yielded a ribozyme that catalyzes RNA polymerization in short stretches (Ekland and Bartel, 1996). RNA catalysis is not restricted to operating on RNA, nor do nucleic acid catalysts require the ribose backbone. Ribozymes were trained by evolutionary techniques to process DNA rather than their natural RNA substrate (Beaudry and Joyce, 1992), and catalytically active DNA molecules were evolved as well (Breaker and Joyce, 1994; Cuenoud and Szostak, 1995). Polynucleotide kinase activity of ribozymes has been reported (Lorsch and Szostak, 1994, 1995) as well as self-alkylation of RNA on nitrogen (Wilson and Szostak, 1995).

Systematic studies have also revealed examples of RNA catalysis on non-nucleic acid substrates. RNA catalyzes ester, amino acid, and peptidyltransferase reactions (Lohse and Szostak, 1996; Zhang and Cech, 1997; Jenne and Famulok, 1998). The latter examples are particularly interesting because they revealed close similarities between the RNA catalysis of peptide bond formation and ribosomal peptidyltransfer (Zhang and Cech, 1998). A spectacular finding in this respect was that oligopeptide bond cleavage and formation is catalyzed by ribosomal RNA and not by protein: More than 90% of the protein fraction can be removed from ribosomes without losing the catalytic effect on peptide bond formation (Noller *et al.*, 1992; Green and Noller, 1997). These experiments found a straightforward interpretation in the atomic structure of the ribosome (Ban *et al.*, 2000; Nissen *et al.*, 2000). In addition, ribozymes were prepared that catalyze alkylation on sulfur atoms (Wecker *et al.*, 1996) and, finally, RNA molecules were designed that are catalysts for typical reactions of organic chemistry, for example an isomerization of biphenyl derivatives (Prudent *et al.*, 1994). A ribozyme with $Zn^{\oplus}$ and NADH as coenzyme was active in a redox reaction with an aldehyde substrate (Tsukiji *et al.*, 2004). A particularly interesting case is a ribozyme catalyzing the Diels-Alder reaction (Seelig and Jäschke, 1999; Serganov *et al.*, 2005), an organic reaction during which two new carbon–carbon bonds are formed.

For two obvious reasons RNA was chosen to be the preferred candidate for the leading molecule in a scenario at the interface between

chemistry and biology: (1) RNA is capable of storing retrievable information, because it is an obligatory replicon, and (2) it has widespread catalytic properties. Although the catalytic properties of RNA are more modest than those of proteins, they are apparently sufficient for processing RNA. RNA molecules operating on RNA molecules form a self-organizing system that can develop molecular organizations with emerging properties and functions. This scenario has been termed the RNA world (see, e.g., Gilbert, 1986; Joyce, 1991, as well as the collective volume by Gesteland and Atkins, 1993, and the recent update, Gesteland *et al.*, 2006). The idea of an RNA world turned out to be fruitful in a different aspect too—it initiated the search for molecular templates and created an entirely new field that may be characterized as template chemistry (Orgel, 1992). Series of systematic studies were performed, for example, on the properties of nucleic acids with modified sugar moieties (Eschenmoser, 1993). These studies revealed the special role of ribose and provided explanations why this molecule is basic to all information-based processes in life.

Chemists working on origin of life problems envisage a number of difficulties for an RNA world being a plausible direct successor of the functionally unorganized prebiotic chemistry (see Figure 1.1 and the reviews by Orgel, 1987, 1992, 2003; Joyce, 1991; Schwartz, 1997): (1) no convincing prebiotic synthesis for all RNA building blocks under the same conditions has been demonstrated, (2) materials for successful RNA synthesis require a high degree of purity that can hardly be achieved under prebiotic conditions, (3) RNA is a highly complex molecule whose stereochemically correct synthesis (3′-5′ linkage) requires an elaborate chemical machinery, and (4) enzyme-free template-induced synthesis of RNA molecules from monomers has not been achieved so far. In particular, the dissociation of duplexes into single strands and the optical asymmetry problem are of major concern. Template-induced synthesis of RNA molecules requires pure optical antipodes. Enantiomeric monomers (containing L-ribose instead of the natural D-ribose) are "poisons" for the polycondensation reaction on the template since their incorporation causes termination of the polymerization process. Currently no plausible conditions are known that could lead to a source of sufficiently pure chiral molecules.[2]

Several suggestions postulating other "intermediate worlds" between chemistry and biology preceding the RNA world have been made. Most of the intermediate information carriers were thought to be more primitive and easier to synthesize than RNA but nevertheless still have the capability of template action (Schwartz, 1997). Glycerol, for example, was suggested as a substitute for ribose because it is structurally simpler and it lacks chirality. However, no successful attempts to use such less sophisticated backbone molecules together with the natural purine and pyrimidine bases for template reactions have been reported so far.

Starting from an RNA world with replicating and catalytically active molecules, it took a long series of many not yet understood steps to arrive at the first cellular organisms with organized cell division and metabolism (see Eigen and Schuster, 1982; Maynard Smith and Szathmáry, 1995). These first precursors of our present-day bacteria and archaea presumably formed the earliest identified fossils (Warrawoona, Western Australia, 3.4×10^9 years old; Schopf, 1993; see Figure 1.1) and/or eventually also the even older kerogen found in the Isua formation (Greenland, 3.8×10^9 years old; Pflug and Jaeschke-Boyer, 1979; Schidlowski, 1988). The correct interpretation of these microfossils as remnants of early forms of life has been questioned (Brasier *et al.*, 2002), although a recent careful consideration of all available information seems to justify the original interpretation (Schopf, 2006).

[2] It is worth noting in this context that an organic reaction has been discovered (Soai *et al.*, 1995) that follows a mechanism for autocatalytic production of optically almost pure chiral material (Frank, 1953); this had been predicted almost 40 years earlier.

REPLICATION AND COUPLING TO ENVIRONMENT

Autocatalysis in Closed and Open Systems

The simple autocatalytic replication reaction according to the overall mechanism 1 is presented here first, because it allows for the derivation of analytical solutions or for complete qualitative analysis. It serves as a simple model for correct replication. First, we consider replication in a closed system (Figure 1.5),[3] where a uniquely defined equilibrium state is approached after a sufficiently long time.[4] Open chemical systems are required to prevent reaction from the approach towards thermodynamic equilibrium. We consider here two examples: (1) a flow reactor (Figure 1.6) and (2) a reaction vessel called a photocell, which allows for coupling of replicon kinetics to a photochemical reaction (Figure 1.7).

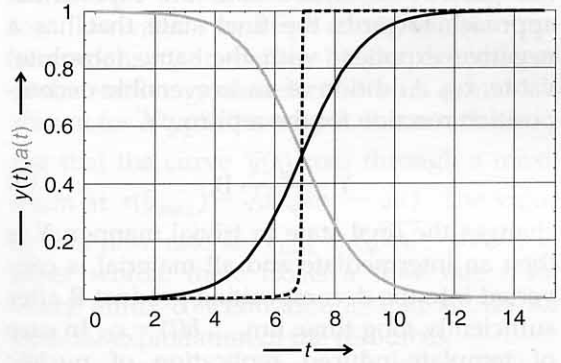

FIGURE 1.5 Replication in a closed system. The figure shows plots of the concentration of the replicator Y (full black line) and the substrate A (gray) as functions of time, $y(t)$ and $a(t)$, respectively, for simple (first order) autocatalysis according to equations (1,1b). Second order autocatalysis (27) leads to the steep curve (broken black line). The curves were adjusted to yield $y = 0.5$ for $t = 6.907$. Choice of parameters: $a(0) = a_0 = 0.999$, $x(0) = x_0 = 0.001$ in arbitrary concentration units (m), $k = 1$ ($m^{-1}t^{-1}$) and $k = 145.35$ ($m^{-2}t^{-1}$) for simple and second order catalysis.

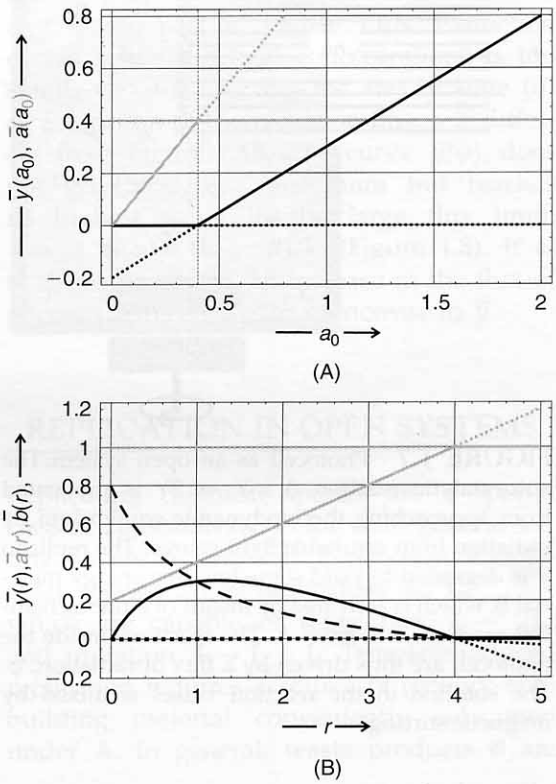

FIGURE 1.6 Replication in a flow reactor. (A) The stationary concentrations $\bar{y}$. (black lines) and $\bar{a}$ (gray lines) as functions of the influx concentration of A, a_0. For the parameter choice applied here we have $\bar{b} = \bar{y}$. Unstable stationary states are shown as dotted lines. A transcritical bifurcation is observed at $a_0 = 0.4$ (m). (B) The stationary concentrations $\bar{y}$. (full black curve), $\bar{a}$ (gray line) and $\bar{b}$ (broken black line) as functions of the flow rate r. Choice of parameters: $k = 5$ ($m^{-1}t^{-1}$), $d = 1$ (t^{-1}).

[3] A closed system exchanges heat but no materials with the environment. A typical example is an isothermal reaction at constant pressure in a closed reaction vessel.

[4] Equation (1) is not correct in the strict sense of thermodynamics, because the reverse reaction, $2Y \rightarrow A + Y$, is not considered explicitly. In order to make the mechanism formally correct the reverse reaction needs to be added, commonly with a (negligibly) small rate constant that makes the analysis a bit more involved but does not change any result or conclusion derived here.

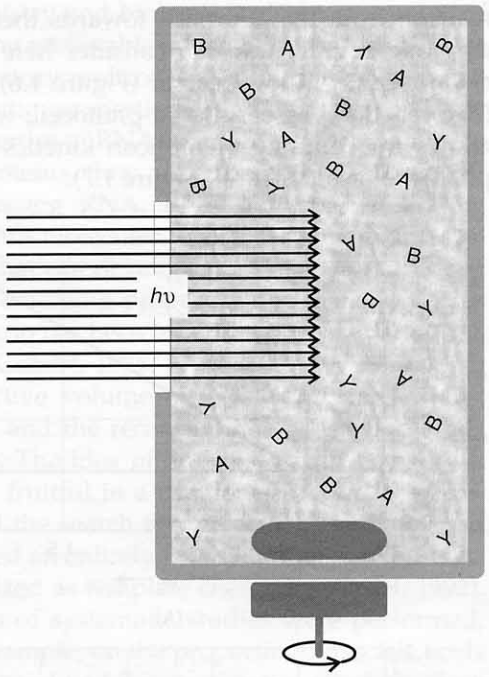

FIGURE 1.7 Photocell as an open system. The autocatalytic reaction A + Y → 2Y is prevented from approaching thermodynamic equilibrium by radiation from a suitable light source. The replicon Y is degraded to yield some low free energy material B, which is activated by means of a photochemical reaction, B + $h\nu$ → A. The reactions inside the photocell are thus driven by a flux of radiation, φ. The solution in the reaction vessel is mixed by magnetic stirring.

Autocatalysis in the closed system is described by the rate equation (concentrations are denoted by lower case letters $a = (A)$ and $y = (Y)$):

$$-\frac{da}{dt} = -\dot{a} = \frac{dy}{dt} = \dot{y} = k\,a \cdot y, \qquad (1a)$$

mass conservation, $a(t) + y(t) = a(0) + y(0) = c_0$ (where c_0 is the total concentration), and initial conditions, $a(0) = a_0$ and $y(0) = y_0$. An analytical solution is computed straightforwardly,

$$y(t) = \frac{y_0 c_0}{y_0 + a_0 e^{-kc_0 t}}, \qquad (1b)$$

and shows the expected behavior in the limits

$$\lim_{t \to o} y(t) = y_0 \text{ and } \lim_{t \to \infty} y(t) = c_0.$$

In other words, all material **A** is converted into **Y** in the long time limit.[5] For $a_0 \gg y_0$ and small t we obtain for the time dependence of the concentration of Y,

$$y(t) \approx y_0 \cdot e^{kc_0 \cdot t} \text{ for small } t,$$

corresponding to exponential growth of the replicon:

$$y(t) \approx c_0 \left(1 - \frac{a_0}{y_0} e^{-kc_0 \cdot t}\right) \text{ for large } t.$$

As shown in Figure 1.5 by means of a numerical example, the initial phase of exponential growth is turned into an exponential approach towards the final state that has a negative exponent with the same (absolute) value, kc_0. Addition of an irreversible decomposition reaction for the replicon Y,

$$\mathrm{Y} \xrightarrow{d} \mathrm{B}, \qquad (5)$$

changes the final state in trivial manner: **Y** is then an intermediate and all material is converted into the decomposition product **B** after sufficiently long time: $\lim_{t \to \infty} b(t) = c_0$. In case of template-induced replication of nucleic acids, for example, A would be the activated monomers, the trinucleotides, whereas B stands for the mononucleotides.

Autocatalysis in the flow reactor considering replication and degradation follows the mechanism

$$\begin{aligned} * &\xrightarrow{a_0 \cdot r} \mathrm{A} \\ \mathrm{A} + \mathrm{Y} &\xrightarrow{k} 2\mathrm{Y} \\ \mathrm{Y} &\xrightarrow{d} \mathrm{B} \\ \mathrm{A},\,\mathrm{B},\,\mathrm{Y} &\xrightarrow{r} \varnothing, \end{aligned} \qquad (6)$$

[5] This is a consequence of the assumption that reaction (1) is irreversible.[4] In case the inverse reaction of (1) would be included with a non-zero rate constant the system would approach an equilibrium state at infinite time, which is defined by $\bar{x}/\bar{a} = K$, where K is the equilibrium parameter of the reaction (1).

and is described by the following kinetic differential equation

$$\begin{aligned} \dot{a} &= -kay + r(a_0 - a), \\ \dot{y} &= (ka - (d + r))\, y \text{ and} \\ \dot{b} &= dx - rb. \end{aligned} \tag{7}$$

The reaction sustains two stationary states: (i) the state of extinction $\bar{a} = a_0$, $\bar{x} = 0$, $\bar{b} = 0$, and (ii) the active state:

$$\begin{aligned} \bar{a} &= \frac{d + r}{k}, \; \bar{x} = \frac{ka_0 - (d + r)}{k(d + r)}\, r, \\ \bar{b} &= \frac{ka_0 - (d + r)}{k(d + r)}\, d. \end{aligned} \tag{7a}$$

The two scenarios are separated by a transcritical bifurcation: The active state is stable at $r < ka_0 - d$ and this implies at sufficiently low flow rates r or large enough influx concentrations a_0. In Figure 1.6 the dependence of the stationary concentrations on a_0 and r is shown for a typical example. It is worth noticing that the curve $\bar{y}(r)$ goes through a maximum at $r(\bar{y}_{\max}) = \sqrt{d}(\sqrt{ka_0} - \sqrt{d})$. The value at this flow rate is: $\bar{y}_{\max} = (\sqrt{ka_0} - d)^2/k$. In other words, there exists a flow rate r for every influx concentration a_0 that allows for optimal exploitation of the resources.

Autocatalysis in the photocell is driven by a flux of photons, which are consumed in a (recycling) photoreaction according to the mechanism

$$\begin{aligned} \mathbf{A} + \mathbf{Y} &\xrightarrow{k} 2\mathbf{Y} \\ \mathbf{Y} &\xrightarrow{d} \mathbf{B} \\ h\nu + \mathbf{B} &\xrightarrow{\varphi} \mathbf{A}, \end{aligned} \tag{8}$$

which gives rise to the differential equation

$$\begin{aligned} \dot{a} &= -kay + \varphi b, \\ \dot{y} &= (ka - d)y \text{ and} \\ \dot{b} &= dx - \varphi b. \end{aligned} \tag{9}$$

Therefore the system shows mass conservation, $a(t) + y(t) + b(t) = a_0$ and one variable can be eliminated: $b(t) = a_0 - a(t) - y(t)$. There are two steady states: (i) extinction, $\bar{a} = a_0$, $\bar{y} = b = 0$, and (ii) the active state:

$$\bar{a} = \frac{d}{k}, \; \bar{y} = \frac{ka_0}{k(d + \varphi)}\, \varphi, \; \bar{b} = \frac{ka_0}{k(d + \varphi)}\, d.$$

The dependence of the stationary concentration on the total concentration is in full analogy to the plot in Figure 1.6A. Extinction occurs when the total concentrations is too small, $a_0 < d/k$. Plotting the steady state (ii) as a function of the radiation flux φ is different from Figure 1.6B: The curve $\bar{y}(\varphi)$, does not go through a maximum but reaches its highest value in the large flux limit, $\lim_{\varphi \to \infty} \bar{y}(\varphi) = (ka_0 - d)/k$ (Figure 1.8). If a_0 is above threshold, an increase in the flux of photons leads always to an increase in $\bar{y}$.

REPLICATION IN OPEN SYSTEMS

Replicating chemical species are a special class of autocatalysts. In the most general setting, we are dealing with a collection of molecular species called replicators $\{\mathbf{I}_1, \mathbf{I}_2, \ldots\}$, which are capable of replication, $\mathbf{I}_k \rightarrow 2\mathbf{I}_k$, and mutation, $\mathbf{I}_j \rightarrow \mathbf{I}_k + \mathbf{I}_j$. Template-induced replication requires a source of (energy-rich) building material conveniently subsumed under **A**. In general, waste products **B** are

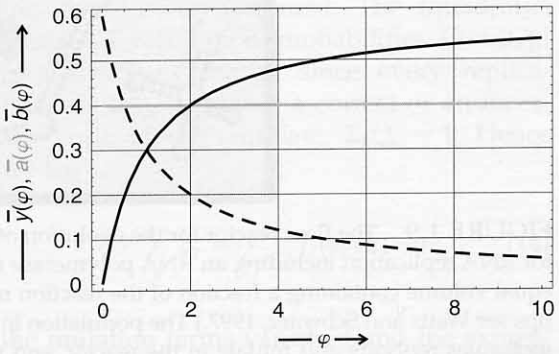

FIGURE 1.8 Steady state in the photocell. The concentrations in the steady state, $\bar{y}$ (black, full line), $\bar{a}$ (gray), and $\bar{b}$ (black, broken line), are plotted as functions of the radiation flux φ. Choice of parameters: $a_0 = 1(m)$, $k = 1(m^{-1}t^{-1})$, and $d = 1(t^{-1})$.

produced through a degradation process. They can be neglected unless they interact further with the replicators or they are recycled. We shall discuss two examples of open systems, the flow reactor (Figure 1.9), where degradation products can be neglected, and the photocell (Figure 1.7), which recycles the degradation products through a photochemical reaction (8). The state of the system and its evolution are conveniently described by time-dependent concentrations of replicators $\mathbf{c}(t) = (c_1(t), c_2(t), \ldots)$ and building blocks $a(t)$, which are determined by initial conditions and kinetic differential equations.

In the flow reactor the ordinary differential equation is of the form:

$$\begin{aligned} \dot{c}_k &= G_k(a, \mathbf{c}) - r\, c_k\,, \; k = 1, 2, \ldots \\ \dot{a} &= r\,(a_0 - a) - \sum_j G_j(a, \mathbf{c})) \end{aligned} \tag{10}$$

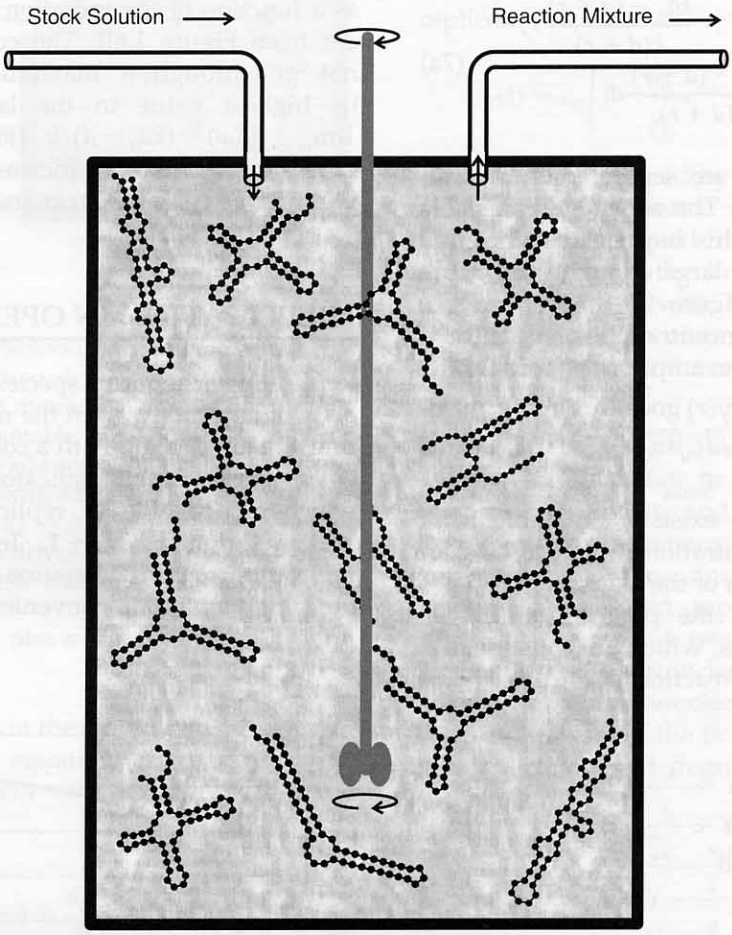

FIGURE 1.9 The flow reactor for the evolution of RNA molecules. A stock solution containing all materials for RNA replication including an RNA polymerase flows continuously into a well-stirred tank reactor and an equal volume containing a fraction of the reaction mixture leaves the reactor. (For different experimental setups see Watts and Schwarz, 1997.) The population in the reactor fluctuates around a mean value, $N \pm \sqrt{N}$. RNA molecules replicate and mutate in the reactor, and the fastest replicators are selected. The RNA flow reactor has been used also as an appropriate model for computer simulations (Fontana and Schuster, 1987; Huynen *et al.*, 1996; Fontana and Schuster, 1998a). There, other criteria than fast replication can be used for selection. For example, fitness functions are defined that measure the distance to a predefined target structure and fitness increases during the approach towards the target (Huynen *et al.*, 1996; Fontana and Schuster, 1998a).

The replication functions G_k reflect the kinetics of the mechanism of reproduction and may be highly complex. In case degradation according to (6) is important, the term $-d_k \cdot c_k$ is properly included in the replication function. A differential equation for the total concentration $c = \sum_k c_k$ is derived by summation,

$$\sum_k \dot{c}_k = \dot{c} = \sum_k G_k - rc = \sum_k G_k - \phi(t), \quad (11)$$

where $\phi(t)$ is a concentration weighted generalized flux representing the material flowing out of the reactor. For constant total concentration denoted as constant organization we have $\dot{c} = 0$ and obtain a condition for this flux: $\phi(t) = \Sigma_k G_k$, which implies an adjustable flux $r(t) = \Sigma_k G_k / c$.

Equation (11) has the formal solution

$$c(t) = c(0) + \int_0^t \left(\sum_k G_k - \phi(\tau) \right) d\tau.$$

emphasizing the time-dependence of the total concentration $c(t)$ in the general case. Introducing normalized concentrations for the replicators, $x_k = c_k / c$ and computing their time derivatives

$$\dot{x}_k = \frac{1}{c}(\dot{c}_k - x_k \dot{c}),$$

results in a system of equations for internal equilibration that does not depend explicitly on the flow rate r:

$$\dot{x}_k = \frac{1}{c(t)} \left(G_k(c\mathbf{x}) - x_k \sum_j G_j(c\mathbf{x}) \right). \quad (12)$$

The expression becomes particularly handy if the replication functions G_k are homogeneous in the concentrations c_k, for example—in the simplest case—polynomials of degree λ, $G_k(\mathbf{c}) = c\lambda \cdot G_k(\mathbf{x})$:[6]

$$\dot{x}_k = c(t)^{\lambda - 1} \left(G_k(\mathbf{x}) - x_k \sum_j G_j(\mathbf{x}) \right).$$

As long as the total concentration does not vanish (and stays finite), the function $c(t)$ can be absorbed in the time axis. In other words, the survival of the entire system requires that c stays bounded away from 0 for all times. According to equation (11) the balance of the intrinsic net production $\Sigma_k G_k$ and the external dilution flux $r(t)$ determines the survival of the entire system. The internal equilibrium is approached independently of the setup of the particular open system applied. If the reactions of interest are modeled by one-step template-induced replication reactions, the functions G_k are of the form $G_k(a, \mathbf{c}) = c_k f_k(a)$, $\lambda = 1$, and equation (12) is exact in real time, i.e. without the time transforming factor involving c.

In a more general setting, incorrect replication is allowed. This can be described by specifying the probabilities Q_{kj} that a copy of type $\mathbf{I}_k$ is produced from a template of type $\mathbf{I}_j$: $G_k = \Sigma_j Q_{kj} f_j(a) c_j$. In this case, the first line of equation (10) can be rewritten in the form

$$\dot{c}_k = \sum_j Q_{kj} c_j f_j(a, c\mathbf{x}) - rc_k \quad (13)$$

where f_j is a growth rate that depends on the chemical environment. The (quadratic) matrix of replication probabilities $Q = \{Q_{kj}\}$ is a stochastic matrix since every replication has to yield either a correct or an incorrect copy of the template, $\Sigma_k Q_{kj} = 1$. Hence we have,

$$\dot{c} = \sum_k \dot{c}_k = \sum_j c_j f_j(a, c\mathbf{x}) - rc, \quad (14)$$

the mutation terms vanished and the expression for $\dot{c}$ is the same as in case of error-free replication.

For relative concentrations, x_k, a short computation shows that mutual relationship of

[6] The condition of homogeneous replication functions is very often fulfilled when the mechanism of replication is the same for all replicators.

the replicators is described by a differential equation of the form

$$\dot{x}_k = \underbrace{x_k\left[f_k(a,c\mathbf{x}) - \sum_j x_j f_j(a,c\mathbf{x})\right]}_{\text{selection}} + \underbrace{\sum_j \{Q_{kj}x_j f_j(a,c\mathbf{x}) - Q_{jk}x_k f_k(a,c\mathbf{x})\}}_{\text{mutation}} \tag{15}$$

In the special case in which $r(t)$ is adjusted such that c stays constant, it can be absorbed into the definition of f_j and it is sufficient to consider the internal competition of the replicons.

For replication in the photocell the flow rate r is replaced by the degradation rate parameter d_k in equation (10) and the production term in the equation for $\dot{a}$, $r(a_0 - a)$ is exchanged for $\varphi \cdot [\mathbf{B}] = \varphi \cdot b = \varphi \cdot (a_0 - a - c)$:

$$\begin{aligned}\dot{c}_k &= G_k(a,\mathbf{c}) - d_k c_k\,, \quad k = 1, 2, \ldots \\ \dot{a} &= \varphi(a_0 - a - c) - \sum_j G_j(a,\mathbf{c})).\end{aligned} \tag{16}$$

Defining $\Gamma_k(a,\mathbf{c}) = G_k(a,\mathbf{c}) - d_k c_k$ we obtain for the internal equilibration an expression that is identical with equation (12) except G is replaced by Γ. For simple replication, $\lambda = 1$, we have $\dot{c}_k = c_k(f_k(a) - d_k) = c_k \cdot \gamma_k$ and internal equilibration is described by

$$\dot{x}_k = \gamma_k x_k - x_k \sum_j \gamma_j x_j \text{ with } \gamma_k = f_k(a) - d_k.$$

The introduction of mutation following exactly the same derivation as before is straightforward.

The mathematical derivations above can be summarized as follows:

- The competition of replicators for common resources can be formulated in terms of relative concentrations. Both their total concentration c and the concentration a of the building material enter only as "parameters" into the associated growth rate functions f_k. In particular, if the vector field f is a homogeneous function in c and a, i.e., if $f_k(a,c\mathbf{x}) = a^p c^q f_k(1,\vec{x})$ for all k, then one can absorb the common prefactor $a^p c^q$ into a rescaling of the time axis (Schuster and Sigmund, 1985). In this case, the internal dynamics of the replicators becomes completely independent of the environment. In the limit of small fluxes, the flow reactor and constant organization yield essentially the same results even for non-homogeneous interaction functions (Happel and Stadler, 1999).
- Selection acting of correct copies and the effects of miscopying can be separated into additive contributions. Indeed, the term in the curly brackets disappears when the matrix $\mathbf{Q}$ is diagonal. Since $\mathbf{Q}$ is a stochastic matrix by definition, the time dependence of the total concentration, $\dot{c}$, is independent of mutation terms. In other words, the internal production does not depend on the mutations matrix $\mathbf{Q}$.
- The overall survival of the system in the flow reactor is governed by the balance between the external dilution flux r and the internal production ϕ. In case of the photocell a minimum amount of material is required for survival according to the condition for the active state (ii) derived from equation (9).

REPLICATION IN LIPID AGGREGATES

These observations remain valid in even more general settings. We consider here an example. Cavalier-Smith (2001) discussed a model for the origin of life in which membranes initially functioned as supramolecular structures to which different replicators attached. In this picture, the membranes are selected as a higher level reproductive unit. From a biophysical point of view, this model is simpler than micellar or vesicular protocells since it avoids the difficulties of modeling the regulation of both growth and fission. More precisely, the "pre-protocell" in Figure 1.10, consists of a lipid aggregate that can grow by inclusion of amphiphilic molecules from the environment. Attached to its surface is a suitable nucleic acid analogue that undergoes uncatalyzed replication in the spirit of the membrane linked replication cycle of the "Los Alamos Bug" (Rasmussen *et al.*, 2003, 2004a).

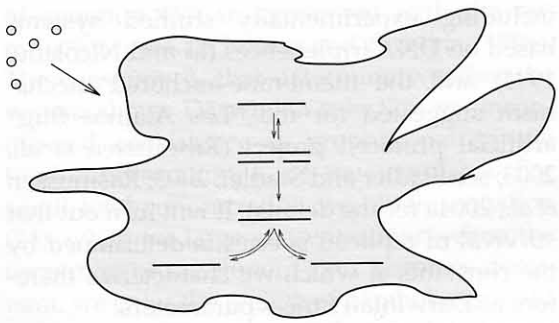

FIGURE 1.10 Model of a protocell precursor. Replicating polymers are attached to the surface of a lipid aggregate which can grow by incorporating amphiphilic molecules from the environment.

The dynamical properties of this model are discussed in some detail in Stadler and Stadler (2007). Suppose the number n_{ka} of replicators of type k embedded in membrane fragment a grows according to the $\dot{n}_{ka} = n_{ka} f_k(\mathbf{c}_a)$ where $\mathbf{c}_a$ is the vector of replicator concentrations in membrane a. Denoting the surface area of the membrane by Ω_a we can write $c_{ka} = n_{ka}/\Omega_a$. A short computation again leads to an equation of the same form as equation (15) for the relative concentrations $x_{ka} = c_{ka}/c_a$ of replicators within each piece of membrane. Furthermore we obtain a set of equations describing to total concentrations c_a of replicators within a given membrane.

$$\dot{c}_a = c_a \sum_j x_j f_j(c_a \cdot \mathbf{x}_a) - c_a \frac{\dot{\Omega}_a}{\Omega_a} \qquad (17)$$

Note that c_a now explicitly depends on the growth law for the membrane itself, i.e. to complete the model we now need to explicitly describe the membrane growth $\dot{\Omega}_a$.

PARABOLIC AND EXPONENTIAL GROWTH

It is relatively easy to derive a kinetic rate equation displaying the elementary behavior of replicons if one assumes (i) that catalysis proceeds through the complementary binding of reactant(s) to free template and (ii) that autocatalysis is limited by the tendency of the template to bind to itself forming an inactive dimer in the manner of product inhibition (von Kiedrowski, 1993). However, in order to achieve an understanding of what is likely to happen in systems where there is a diverse mixture of reactants and catalytic templates, it is desirable to develop a comprehensive kinetic description of as many individual steps in the reaction mechanism of template synthesis as is feasible and tractable from the mathematical point of view.

Szathmáry and Gladkih (1989) over-simplified the resulting dynamics to a simple parabolic growth law $\dot{x}_k \propto x_k^p$, $0 < p < 1$ for the concentrations of the interacting template species. This model suffers from a conceptual and a technical problem: (i) under no circumstances does one observe extinction of a species in any parabolic growth model, and (ii) the vector fields are not Lipschitz-continuous on the boundary of the concentration simplex, indicating that we cannot expect uniqueness of solutions, and thus that we cannot take for granted that the system behaves physically reasonable in this area.

In Wills *et al.* (1998), we have derived the kinetic equations for a system of coupled template-instructed ligation reactions of the form

$$\begin{aligned} &\mathbf{A}_i + \mathbf{B}_j + \mathbf{C}_{kl} \underset{\bar{a}_{ijkl}}{\overset{a_{ijkl}}{\rightleftharpoons}} \mathbf{A}_i\mathbf{B}_j\mathbf{C}_{kl} \\ &\xrightarrow{b_{ijkl}} \mathbf{C}_{ij}\mathbf{C}_{kl} \underset{\bar{d}_{ijkl}}{\overset{d_{ijkl}}{\rightleftharpoons}} \mathbf{C}_{ij} + \mathbf{C}_{kl} \end{aligned} \qquad (18)$$

Here **A**. and **B**. denote the two substrate molecules which are ligated on the template **C**.., for example, the electrophilic, **E**, and the nucleophilic, **N**, oligopeptide in peptide template reactions or the two different trinucleotides, **GGC** and **GCC**, in the autocatalytic hexanucleotide formation (Figure 1.2). This scheme thus encapsulates the experimental results on both peptide and nucleic acid replicons (von Kiedrowski, 1986; Lee *et al.*, 1996).

The following assumptions are straightforward and allow for a detailed mathematical analysis:

(i) the concentrations of the intermediates are stationary in agreement with the "quasi-steady state" approximation (Segel and Slemrod, 1989),

(ii) the total concentration c_0 of all replicating species is constant in the sense of constant organization (Eigen, 1971),

(iii) the formation of heteroduplices of the form $\mathbf{C}_{ij}\mathbf{C}_{kl}$, $ij \neq kl$ is neglected, and
(iv) only reaction complexes of the form $\mathbf{A}_k\mathbf{B}_l\mathbf{C}_{kl}$ lead to ligation.

Assumptions (iii) and (iv) are closely related. They make immediate sense for hypothetical macromolecules for which the template instruction is direct instead of complementary. It has been shown, however, that the dynamics of complementary replicating polymers is very similar to direct replication dynamics if one considers the two complementary strands as "single species" by simply adding their concentrations (Eigen, 1971; Stadler, 1991).

Assumptions (iii) and (iv) suggest a simplified notation of the reaction scheme:

$$\begin{aligned} \mathbf{A}_k + \mathbf{B}_k + \mathbf{C}_k &\underset{\bar{a}_k}{\overset{a_k}{\rightleftharpoons}} \mathbf{A}_k\mathbf{B}_k\mathbf{C}_k \\ &\xrightarrow{b_k} \mathbf{C}_k\mathbf{C}_k \underset{\bar{d}_k}{\overset{d_k}{\rightleftharpoons}} 2\mathbf{C}_k \end{aligned} \tag{19}$$

It can be shown that equation (19) together with the assumptions (i) and (ii) leads to the following system of differential equations for the frequencies or relative total concentrations x_k, i.e. $\sum_k^m x_k = 1$ of the template molecules $\mathbf{C}_k$ in the system (note that x_k accounts not only for the free template molecules but also for those bound in the complexes $\mathbf{C}_k\mathbf{C}_k$ and $\mathbf{A}_k\mathbf{B}_k\mathbf{C}_k$):

$$\dot{x}_k = x_k\left(\alpha_k\varphi(c\beta_k x_k) - \sum_j^m \alpha_j x_j \varphi(c\beta_j x_j)\right), \quad k = 1, \ldots, m, \tag{20}$$

where

$$\varphi(z) = \frac{2}{z}\left(\sqrt{z+1} - 1\right) \quad \varphi(0) = 1, \tag{21}$$

and the effective kinetic constants α_k and β_k can be expressed in terms of the physical parameters a_k, $\bar{a}_k$, etc. This special form of the growth rate function,

$$f_k(c, \vec{x}) = \alpha_k\varphi(c\beta_k x_k) \tag{22}$$

is also obtained from a wide range of alternative template-directed ligation mechanisms, including experimentally studied systems based on DNA triplehelices (Li and Nicolaou, 1994) and the membrane-anchored mechanism suggested for the "Los Alamos Bug" artificial protocell project (Rasmussen *et al.*, 2003; see Stadler and Stadler, 2003; Rasmussen *et al.*, 2004a for the details). It will turn out that survival of replicon species is determined by the constants α_k which we characterize therefore as Darwinian fitness parameters.

Equation (20) is a special form of a replicator equation with the non-linear response functions $f_k(x) := \alpha_k\varphi(\beta_k x_k)$. Its behavior depends strongly on the values of β_k: For large values of z we have $\varphi(z) \sim 2/\sqrt{z}$. Hence equation (20) approaches Szathmáry's expression (Szathmáry and Gladkih, 1989):

$$\dot{x}_k = h_l\sqrt{x_k} - x_k\sum_j^M h_j\sqrt{x_j} \tag{23}$$

with suitable constants h_k. This equation exhibits a very simple dynamics: the mean fitness $\Phi(x) = \sum_j^M h_j\sqrt{x_j}$ is a Ljapunov function, i.e. it increases along all trajectories, and the system approaches a globally stable equilibrium at which all species are present (Wills *et al.*, 1998; Varga and Szathmáry, 1997). Szathmáry's parabolic growth model thus does not lead to selection.

On the other hand, if z remains small, that is, if β_k is small, then $\varphi(\beta_k x_k)$ is almost constant 1 (since the relative concentration x_k is of course a number between 0 and 1). Thus we obtain

$$\dot{x}_k = x_k\left(\alpha_k - \sum_j^M \alpha_j x_j\right) \tag{24}$$

which is the "no-mutation" limit of Eigen's kinetic equation for replication (Eigen, 1971) (see equation (33a); if condition (iv) above is relaxed, we in fact arrive at Eigen's model with a mutation term). Equation (24) leads to survival of the fittest: The species with the largest value of α_k will eventually be the only survivor in the system. It is worth noting that the mean fitness also increases along all orbits

of equation (24) in agreement with the no-mutation case (Schuster and Swetina, 1988). The constants β_k that determine whether the system shows Darwinian selection or unconditional coexistence is proportional to the total concentration c_0 of the templates. For small total concentration we obtain equation (24), while for large concentrations, when the formation of the dimers $\mathbf{C}_k\mathbf{C}_k$ becomes dominant, we enter the regime of parabolic growth.

Equation (20) is a special case of a class of replicator equations studied by Hofbauer *et al.* (1981). Restating their main result yields the following: All orbits or trajectories starting from physically meaningful points (these are points in the interior of the simplex S_M with $x_j > 0$ for all $j = 1, 2, \ldots, M$) converge to a unique equilibrium point $\bar{\mathbf{x}} = (\bar{x}_1, \bar{x}_2, \ldots, \bar{x}_M)$ with $\bar{x}_i \geqslant 0$, which is called the ω-limit of the orbits. This means that species may go extinct in the limit $t \to \infty$. If $\bar{x}$ lies on the surface of S_M (which is tantamount to saying that at least one component $\bar{x}_j = 0$) then it is also the ω-limit for all orbits on this surface. If we label the replicon species according to decreasing values of the Darwinian fitness parameters, $\alpha_1 \geq \alpha_2 \geq \ldots \geq \alpha_M$, then there is an index $\ell \geq 1$ such that $\bar{\mathbf{x}}$ is of the form $\bar{x}_i > 0$ if $i \leq \ell$ and $\bar{x}_i = 0$ for $i > \ell$. In other words, ℓ replicon species survive and the $M - \ell$ least efficient replicators die out. This behavior is in complete analogy to the reversible exponential competition case (Schuster and Sigmund, 1985) where the Darwinian fitness parameters α_k are simply the rate constants a_k. If the smallest concentration dependent value $\beta_s(c_0) = \min\{\beta_j(c_0)\}$ is sufficiently large, we find $\ell = M$ and no replicon goes extinct ($\bar{\mathbf{x}}$ is an interior equilibrium point).

The condition for survival of species k is explicitly given by:

$$\alpha_k > \Phi(\bar{\mathbf{x}}) \tag{25}$$

It is interesting to note that the Darwinian fitness parameters α_k determine the order in which species go extinct whereas the concentration-dependent values $\beta_k(c_0)$ collectively influence the flux term and hence set the "extinction threshold." In contrast to Szathmáry's model equation, the extended replicon kinetics leads to both competitive selection and coexistence of replicons depending on total concentration and kinetic constants.

HYPERBOLIC GROWTH

In this section we consider second order autocatalysis which is distinguished from simple (or first order) autocatalysis by the stoichiometry 1 : 2 for substrate **A** and autocatalyst **Y**:

$$\mathbf{A} + 2\mathbf{Y} \xrightarrow{k} 3\mathbf{Y}. \tag{26}$$

Although such a reaction step is often used in simple models for chemical oscillators and pattern formation (Turing, 1952; Nicolis and Prigogine, 1977) as well as non-equilibrium phase transitions (Schlögl, 1972), it occurs in reality only in overall kinetics of many step reactions. The notion of hyperbolic growth is derived from the solution curve of the unconstrained system, $\dot{x} = f \cdot x^2$, the solution curve $x(t) = x_0/(1 - x_0 ft)$ is a hyperbola with the time axis as a horizontal asymptote and a vertical asymptote at $t = 2/(x_0 a)$. The kinetic differential equation for (26) in the closed system can be solved exactly but no explicit expression $x(t)$ is available:

$$t = \frac{1}{k\, a_0}\left(\frac{x - x_0}{x x_0} + \frac{1}{a_0}\ln\frac{x(a_0 - x_0)}{x_0(a_0 - x)}\right). \tag{26b}$$

In Figure 1.5 the solutions curves for first and second order autocatalysis are compared. Second order autocatalysis leads to a comparatively long lag phase and an extremely steep increase in concentration. Precisely such a behavior was observed in the early phase of the infection cycle of a bacteriophage in *Escherichia coli* (Eigen *et al.*, 1991).

In contrast to the weakly coupled networks of replicons considered in previous sections, hypercycles (Eigen, 1971; Eigen and Schuster, 1978a) involve specific catalysis beyond mere template instruction (see Figure 1.11). In the

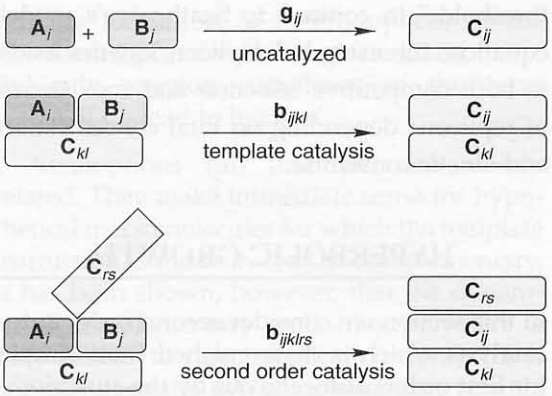

FIGURE 1.11 Modes of template formation. In complex systems of mixed templates and depending on the underlying mechanism of template synthesis, different modes of dynamic behavior are possible. Uncatalyzed synthesis generally corresponds to linear growth. Template-instructed synthesis gives parabolic or exponential growth. The coupling of systems involving second order autocatalysis can also give rise to hyperbolic growth, as has been predicted for hypercycles (Eigen and Schuster, 1978a).

simplest case, where we consider catalyzed replication reactions explicitly, the reaction equations are of the form:

$$(\mathbf{A}) + \mathbf{I}_k + \mathbf{I}_l \rightarrow 2\mathbf{I}_k + \mathbf{I}_l. \tag{27}$$

Here a copy of $\mathbf{I}_k$ is produced using another macromolecular species $\mathbf{I}_l$ as a specific catalyst for the replication reaction. This corresponds to growth rate functions of the form

$$f_k(a, c\mathbf{x}) = \sum_l a_{kl}(a, c)x_l \tag{28}$$

where the matrix $A = \{a_{kl}\}$ describes the network of catalytic interactions. The corresponding kinetic differential equation

$$\dot{x}_k = x_k\left(\sum_l a_{kl}x_l - \phi(\mathbf{x})\right) \tag{29}$$

corresponding to the mechanism (27) has been termed second order replicator equation (Schuster and Sigmund, 1983). These systems can display enormous diversity of dynamic behavior (Hofbauer and Sigmund, 1998).

In case matrix A is diagonal we have $f_k(x) = a_{kk}x_k$, the corresponding dynamical system

$$\dot{x}_k = x_k\left(a_{kk}x_k - \sum_l a_{jj}x_j^2\right) \tag{29a}$$

is known as generalized Schlögl model (Schlögl, 1972; Schuster and Sigmund, 1985): Each replicator considered in isolation shows hyperbolic growth. In the competitive ensemble described by equation (29a) every replicator can be selected, since all pure states corresponding to the corners of the concentration simplex $P_k(S_n) = (x_k = 1,\ x_j = 0\ \forall\ j \neq k)$ are point attractors. Which one is selected depends on the initial conditions. The sizes of the basins of attraction correspond strictly to the values of the replication parameters, i.e. the replicator with the largest a_{kk}-value has the largest basin, the one with the next largest value the next largest basin, etc.

A more realistic version of (27) that might be experimentally feasible is

$$\begin{aligned}
&\mathbf{A}_i + \mathbf{B}_j + \mathbf{C}_{kl} + \mathbf{C}_{rs} \underset{\bar{a}_{ijkl}}{\overset{a_{ijkl}}{\rightleftharpoons}} \mathbf{A}_i\mathbf{B}_j\mathbf{C}_{kl} \\
&+ \mathbf{C}_{rs} \underset{\bar{e}_{ijklrs}}{\overset{e_{ijklrs}}{\rightleftharpoons}} \mathbf{A}_i\mathbf{B}_j\mathbf{C}_{kl}\mathbf{C}_{rs} \xrightarrow{b_{ijklrs}} \\
&\mathbf{C}_{ij}\mathbf{C}_{kl}\mathbf{C}_{rs} \xrightarrow{f_{ijklrs}} \mathbf{C}_{ij} \\
&+ \mathbf{C}_{kl}\mathbf{C}_{rs} \underset{\bar{d}_{ijkl}}{\overset{d_{ijkl}}{\rightleftharpoons}} \mathbf{C}_{ij} + \mathbf{C}_{kl} + \mathbf{C}_{rs}
\end{aligned} \tag{30}$$

Here the template $\mathbf{C}_{rs}$ plays the role of a ligase for the template-directed replication step. Dynamically, it again leads to replicator equations with non-linear growth functions (Stadler *et al.*, 2000). Depending on the total concentration of replicons, they interpolate between a parabolic growth regime, $f_k \sim x_k^{-1/3}$, and hyperbolic growth $f_k \sim x_k$.

Second order replicator equations, equation (29), are mathematically equivalent to Lotka-Volterra equations used in mathematical ecology (Hofbauer, 1981). Indeed, research in the group of John McCaskill (Wlotzka and McCaskill, 1997; McCaskill, 1997) is dealing

with molecular ecologies of strongly interacting replicons.

MOLECULAR EVOLUTION EXPERIMENTS

In the first half of the twentieth century it was apparently out of the question to do conclusive and interpretable experiments on evolving populations on account of two severe problems: (i) time-scales of evolutionary processes are prohibitive for laboratory investigations and (ii) the numbers of possible genotypes are outrageously large and thus only a negligibly small fraction of all possible sequences can be realized and evaluated by selection. If generation times could be reduced to a minute or less, thousands of generations, numbers sufficient for the observation of optimization and adaptation, could be recorded in the laboratory. Experiments with RNA molecules in the test-tube do indeed fulfill this time-scale criterion for observability. With respect to the "combinatorial explosion" of the numbers of possible genotypes the situation is less clear. Population sizes of nucleic acid molecules of 10^{15}–10^{16} individuals can be produced by random synthesis in conventional automata. These numbers cover roughly all sequences up to chain lengths of $n = 27$ nucleotides. These are only short RNA molecules but their length is already sufficient for specific binding to predefined target molecules, for example antibiotics (Jiang *et al.*, 1997) and molecules of similar size, the siRNAs, were found to play an important role in regulation of gene expression (McManus and Sharp, 2002; Mattick, 2004; Marques *et al.*, 2006). Moreover, sequence to structure to function mappings of RNA were found to be highly redundant (Fontana *et al.*, 1993; Schuster *et al.*, 1994) and thus only a small fraction of all sequences has to be searched in order to find solutions to given evolutionary optimization problems.

The first successful attempts to study RNA evolution *in vitro* were carried out in the late 1960s by Sol Spiegelman and his group (Mills *et al.*, 1967; Spiegelman, 1971). They created a "protein assisted RNA replication medium" by adding an RNA replicase isolated from *E. coli* cells infected by the RNA bacteriophage Qβ to a medium for replication that also contains the four ribonucleoside triphosphates (GTP, ATP, CTP, and UTP) in a suitable buffer solution. Qβ RNA and some of its smaller variants start instantaneously to replicate when transferred into this medium. Evolution experiments were carried out by means of the serial transfer technique: Materials consumed in RNA replication are replenished by transfer of small samples of the current solution into fresh stock medium. The transfers were made after equal time steps. In series of up to 100 transfers the rate of RNA synthesis increased by orders of magnitude. The increase in the replication rate occurs in steps and not continuously as one might have expected. Analysis of the molecular weights of the replicating species showed a drastic reduction of the RNA chain lengths during the series of transfers: The initially applied Qβ RNA was 4220 nucleotides long and the finally isolated species contained little more than 200 bases. What happened during the serial transfer experiments was a kind of degradation due to suspended constraints on the RNA molecule. In addition to perform well in replication the viral RNA has to code for four different proteins in the host cell and needs also a proper structure in order to enable packing into the virion. In test-tube evolution these constraints are released and the only remaining requirement for survival are recognition of the RNA by Qβ replicase and fast replication.

Evidence for a non-trivial evolutionary process came a few years later when the Spiegelman group published the results of another serial transfer experiment that gave evidence for adaptation of an RNA population to environmental change. The replication of an optimized RNA population was challenged by the addition of ethidium bromide to the replication medium (Kramer *et al.*, 1974). This dye intercalates into DNA and RNA double helices and thus reduces replication rates. Further serial transfers in the presence of the intercalating substance led to an increase in the replication rate until an

optimum was reached. A mutant was isolated from the optimized population which differed from the original variant by three-point mutations. Extensive studies on the reaction kinetics of RNA replication in the Qβ replication assay were performed by Biebricher (Biebricher and Eigen, 1988). These studies revealed consistency of the kinetic data with many-step reaction mechanism. Depending on concentration the growth of template molecules allows to distinguish three phases of the replication process: (i) at low concentration all free template molecules are instantaneously bound by the replicase which is present in excess and therefore the template concentration grows exponentially, (ii) excess of template molecules leads to saturation of enzyme molecules, then the rate of RNA synthesis becomes constant and the concentration of the template grows linearly, and (iii) very high template concentrations impede dissociation of the complexes between template and replicase, and the template concentration approaches a constant in the sense of product inhibition. We neglect plus–minus complementarity in replication by assuming stationarity in relative concentrations of plus and minus strand (Eigen, 1971) and consider the plus–minus ensemble as a single species. Then, RNA replication may be described by the overall mechanism:

$$\begin{aligned} \mathbf{A} + \mathbf{I}_i + \mathbf{E} &\underset{\bar{k}_i}{\overset{k_i}{\rightleftharpoons}} \mathbf{A} + \mathbf{I}_i \cdot \mathbf{E} \xrightarrow{a_i} \\ \mathbf{I}_i \cdot \mathbf{E} \cdot \mathbf{I}_i &\underset{\bar{k}'_i}{\overset{k'_i}{\rightleftharpoons}} \mathbf{I}_i \cdot \mathbf{E} + \mathbf{I}_i . \end{aligned} \tag{31}$$

Here **E** represents the replicase and **A** stands for the low-molecular-weight material consumed in the replication process. This simplified reaction scheme reproduces all three characteristic phases of the detailed mechanism (Figure 1.12) and can be readily extended to complementary replication and mutation.

Despite the apparent complexity of RNA replication kinetics the mechanism at the same time fulfills an even simpler overall rate law provided the activated monomers, ATP, UTP, GTP, and CTP, as well as Qβ replicase are present in excess. Then, the rate of increase for the concentration x_i of RNA species $\mathbf{I}_i$

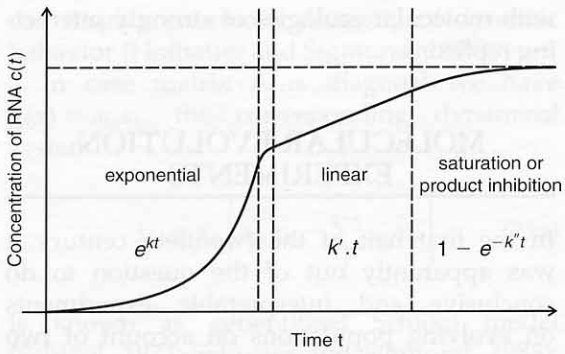

FIGURE 1.12 Replication kinetics of RNA with Qβ replicase. In essence, three different phases of growth are distinguished: (i) exponential growth under conditions with excess of replicase, (ii) linear growth when all enzyme molecules are loaded with RNA, and (iii) a saturation phase that is caused by product inhibition.

follows the simple relation, $\dot{x}_i \propto x_i$, which in absence of constraints ($\phi = 0$) leads to exponential growth. This growth law is identical to that found for asexually reproducing organisms and hence replication of molecules in the test-tube leads to the same principal phenomena that are found with evolution proper. RNA replication in the Qβ system requires specific recognition by the enzyme which implies sequence and structure restrictions. Accordingly only RNA sequences that fulfill these criteria can be replicated. In order to be able to amplify RNA free of such constraints many-step replication assays have been developed. The discovery of the DNA polymerase chain reaction (PCR) (Mullis, 1990) was a milestone towards sequence independent amplification of DNA sequences. It has one limitation: double helix separation requires higher temperatures and therefore conventional PCR works with a temperature program. PCR is combined with reverse transcription and transcription by means of bacteriophage T7 RNA polymerase in order to yield a sequence-independent amplification procedure for RNA. This assay contains two possible amplification steps: PCR and transcription.

Another frequently used assay makes use of the isothermal self-sustained sequence replication reaction of RNA (3SR) (Fahy *et al.*,

1991). In this system the RNA–DNA hybrid obtained through reverse transcription is converted into single-stranded DNA by RNase digestion of the RNA strand, instead of melting the double strand. DNA double strand synthesis and transcription complete the cycle. Here, transcription by T7 polymerase represents the amplification step. Artificially enhanced error rates needed for the creation of sequence diversity in population can be achieved readily with PCR. Reverse transcription and transcription are also susceptible to increase of mutation rates. These two and other new techniques for RNA amplification provided universal and efficient tools for the study of molecular evolution under laboratory conditions and made the use of viral replicases with their undesirable sequence specificities obsolete. Since the 1990s RNA selection experiments have given rise to a new kind of biotechnology making use of evolutionary techniques to create molecules for predefined properties (Klussmann, 2006).

FITNESS LANDSCAPES

So far, we have treated the growth functions f_k as externally given parameters. Only the population dynamics of the replicators $\{\mathbf{I}_1, \mathbf{I}_2, \ldots\}$ has been considered. The function f_k, however, is the mathematical description of the behavior and interactions of a particular chemical entity, the replicator $\mathbf{I}_k$ in a particular environment. In natural evolution, as well as in evolution experiments *in vitro*, mutation (and possibly other mechanisms such as recombination) will cause the emergence of new type of replicons, while existing ones may be driven to extinction by the population dynamics. Thus it is imperative to gain an understanding for the dependence of f_k on the underlying replicons $\mathbf{I}_k$ and to relate this knowledge to the mutual accessibility of variants.

Although the concepts can be generalized further, we restrict ourselves here to the simplest case of constant functions $f_k(\mathbf{x}) = f_k$—we call these fixed values the fitness of $\mathbf{I}_k$—and we assume that our replicons $\mathbf{I}_k$ are sequences of a fixed length n. Sequences can be interconverted by point mutations, hence adjacent sequences differ by a mutation in a single position (it is easy to relax the restriction to point mutations and to include insertions, deletions, and rearrangements into the framework). Let us denote the set of all possible replicon types by Ξ. Given an adjacency relation on Ξ, we can visualize Ξ as a graph, with a adjacent sequences (interrelated by single point mutants) connected by edges.

Fitness can now be seen as a function $f : \Xi \to \mathbb{R}$. Together with the graph structure on Ξ, we speak of a fitness landscape, a concept introduced by Sewall Wright (Wright, 1932) to explain the effect of selection. In the crudest approximation, a population will move in Ξ so as to maximize f. An elaborate mathematical theory has been developed to analyze the structure of fitness landscapes in terms of various measures of ruggedness, i.e. the local variability of fitness values (see Reidys and Stadler, 2001).

Realistic biological fitness landscapes,[7] however, are not just arbitrary functions $f : \Xi \to \mathbb{R}$. In fact, they are naturally decomposed into two steps because it is never the nucleic acid or peptide sequence itself that is subject to selection, but rather the three-dimensional structure that if forms, or the "organism" that it encodes. Hence there is first the map $\Psi : \Xi \to \mathbb{S}$ that connects a sequence with its phenotype, $\mathbf{I}_k \to \Psi(k)$. This phenotype is then "evaluated" by its environment. Hence $f_k = \mathrm{eval}(\Psi(k))$ is a composite of the genotype map Ψ and the fitness evaluation function. In biophysically realistic settings, such as the RNA folding model where the phenotype is by the molecular structure and its properties, one observes substantial redundancy in the genotype-phenotype map, i.e. many genotypes give rise to phenotypes that are indistinguishable. As a consequence, there are many sequences $\mathbf{I}_k \in \Xi$ that have the same fitness. Since in particular closely related sequences are often selectively indistinguishable, there is a certain fraction of neutral mutations

[7] Realistic is used here in order to distinguish these landscapes from oversimplified landscape models often used in population genetics.

with the property that $f_k = f_l$. We shall see below that these neutral mutations play a crucial role in molecular evolution.

Many proposals for simple model landscapes have been made, among them the so-called Nk-landscape of Kauffman (1993) has become very popular. In the simplest realistic case that is based on molecular data, the genotype–phenotype map Ψ is defined by folding the biopolymer sequences (RNA, DNA, or peptide) into its three-dimensional structure. In case of RNA and a simplified notion of structure, the so-called secondary structure the map Ψ is sufficiently simple in order to allow for systematic analysis (Schuster, 2006).

Time-dependent fitness landscapes have been discussed some time ago (see, e.g., Kauffman, 1993; Levitan and Kauffman, 1995). Two major effects introduce dynamics into landscapes: (i) fluctuating environments and (ii) co-evolution. More recently these ideas were extended to a comprehensive treatment of dynamic fitness landscapes (Wilke *et al.*, 2001; Wilke and Ronnewinkel, 2001). Successful application of dynamic landscapes requires that the adaptive process on the landscape occurs on a substantially shorter time-scale than the changes of the landscapes, otherwise strong coupling between adaptation and landscape dynamics makes the landscape concept obscure. In case of co-evolution the separation of time-scales is at least questionable.

QUASISPECIES AND ERROR PROPAGATION

Evolution of molecules based on replication and mutation has been discussed above. Here we consider in detail the internal equilibration in populations as formulated in terms of normalized concentrations (15) and extensively discussed before (Eigen, 1971; Eigen and Schuster, 1977; Eigen *et al.*, 1989). Error-free replication and mutation are seen as parallel chemical reactions,

$$\mathbf{A} + \mathbf{I}_j \xrightarrow{f_j Q_{kj}} \mathbf{I}_k + \mathbf{I}_j, \qquad (32)$$

and constitute a network, which in principle allows for the formation of every RNA genotype as a mutant of any other genotype, $\mathbf{I}_j \rightarrow \mathbf{I}_k$, eventually through a series of consecutive point mutations, $\mathbf{I}_j \rightarrow \mathbf{I}_l \rightarrow \ldots \rightarrow \mathbf{I}_k$. The materials required for or consumed by RNA synthesis, again denoted by A, are kept constant by adjusting flow and influx material in a kind of chemostat (Figure 1.9). The object of interest is now the distribution of genotypes in the population and its dependence on the mutation rate. We shall be dealing here exclusively with single-strand replication but mention a recent approach that considers semi-conservative DNA replication (Tannenbaum *et al.*, 2004, 2006). Spatially resolved reaction-diffusion dynamics of quasispecies has been studied as well (Altmeyer and McCaskill, 2001; Pastor-Satorras and Solé, 2001).

Quasispecies Equation

The time-dependence of the genotype distribution is described by the kinetic equation

$$\dot{x}_k = x_k(f_k Q_{kk} - \phi(t)) + \sum_{j=1, j\neq k}^{m} f_j Q_{kj} x_j, \quad k = 1,\ldots, m. \qquad (33)$$

The replication functions of the molecular species, f_k, are constants under these conditions. The frequencies of the individual reaction channels are contained in the mutation matrix $\mathbf{Q} = \{Q_{kj};\ k, j = 1, \ldots, m\}$. Recall that $\mathbf{Q}$ is a stochastic matrix, $\Sigma_k Q_{kj} = 1$ since every copy is either correct or incorrect.

In the no-mutation limit the mutation matrix $\mathbf{Q}$ is the unit matrix, the kinetic equation has the form

$$\dot{x}_k = x_k(f_k - \phi(t)),\ \ i = 1,\ldots, m \text{ with } \phi(t) = \sum_{j=1}^{m} f_j x_j, \qquad (33a)$$

and an analytical solution of (33a) is available

$$x_k(t) = \frac{x_k(0)\cdot\exp(f_k t)}{\sum_{j=1}^{m} x_j(0)\cdot\exp(f_j t)}. \qquad (33b)$$

The interpretation of the result is straightforward: After sufficiently long time the exponential function with the largest value of the replication rate parameter, $f_M = \max\{f_j;\ j = 1, 2, \ldots, m\}$, dominates the sum in the denominator, and hence $\lim_{t\to\infty} x_M = 1$ and $\lim_{t\to\infty} x_j = 0\ \forall\ j = 1, 2, \ldots, m;\ j \neq M$. The replicator that replicates fastest is selected.

The quantities determining the outcome of selection in the replication–mutation scenario are the products of replication rate constants and mutation frequencies subsumed in the value matrix:[8] $W \doteq \{w_{kj} = f_j Q_{kj};\ k, j = 1, \ldots, m\}$, its diagonal elements, w_{kk}, are called the selective values of the individual genotypes (Eigen, 1971).

The selective value of a genotype is tantamount to its fitness in the case of vanishing mutational backflow and hence the genotype with maximal selective value, $\mathbf{I}_M$,

$$w_{MM} = \max\{w_{kk} \mid i = 1,\ldots,m\} \qquad (34)$$

dominates a population after it has reached the selection equilibrium and is called the master sequence. The notion quasispecies was introduced for the stationary genotype distribution in order to point at its role as the genetic reservoir of an asexual population.

Error Threshold

A simple expression for the stationary frequency can be found if the master sequence is derived from the single peak model landscape that assigns a higher replication rate to the master and identical values to all others, for example $f_M = \sigma_M \cdot f$ and $f_i = f$ for all $i \neq M$ (Swetina and Schuster, 1982; Tarazona, 1992; Alves and Fontanari, 1996). The (dimensionless) factor σ_M is called the superiority of the master sequence. The assumption of a single peak landscape is tantamount to lumping all mutants together into a mutant cloud with average fitness and reminds of a mean field approximation. The probability of being in the cloud is simply $x_c = \sum_{j=1, j\neq M}^{m} x_j = 1 - x_M$ and the replication–mutation problem boils down to an exercise in a single variable, x_M, the frequency of the master. In the sense of a mean field approximation, for example, we define a mean-except-the-master replication rate constant $\bar{f} = \sum_{j\neq M} f_j x_j/(1 - x_M)$. The superiority then reads: $\sigma_M = f_M/\bar{f}$. Neglecting mutational backflow we can readily compute the stationary frequency of the master sequence,

$$\bar{x}_M = \frac{f_M Q_{MM} - \bar{f}}{f_M - \bar{f}} = \frac{\sigma_M Q_{MM} - 1}{\sigma_M - 1}, \qquad (35)$$

which vanishes at some finite replication accuracy, $Q_{MM}|_{\bar{x}_M=0} = Q_{min} = \sigma_M^{-1}$. Non-zero frequency of the master requires $Q_{MM} > Q_{min}$. Within the uniform error rate approximation, which assumes that the mutation rate per site and replication event, p, is independent of the nature of the nucleotide and the position in the sequence (Eigen and Schuster, 1977). Then, the single digit accuracy $q = 1-p$ is the mean fraction of correctly incorporated nucleotides and the elements of the mutation matrix for a polynucleotide of chain length n are of the form:

$$Q_{ij} = q^n \left(\frac{1-q}{q}\right)^{dij},$$

with d_{ij} being the Hamming distance between two sequences $\mathbf{I}_i$ and $\mathbf{I}_j$. The critical condition, called the error threshold, $\bar{x}_M = 0$, occurs at a minimum single digit accuracy of

$$q_{min} = 1 - p_{max} = \sqrt[n]{Q_{min}} = \sigma_M^{-1/n}. \qquad (36)$$

Figure 1.13 shows the stationary frequency of the master sequence, $\bar{x}_M$, as a function of the error rate. The "no mutational backflow approximation" cannot describe how populations behave at mutation rates above the error threshold.

[8] In case degradation rates d_k are important they are readily absorbed in the diagonal terms of the value matrix (Eigen, 1971): $w_{kk} = f_k Q_{kk} - d_k$; see also (16) and the definition of $\Gamma(a, \mathbf{c})$.

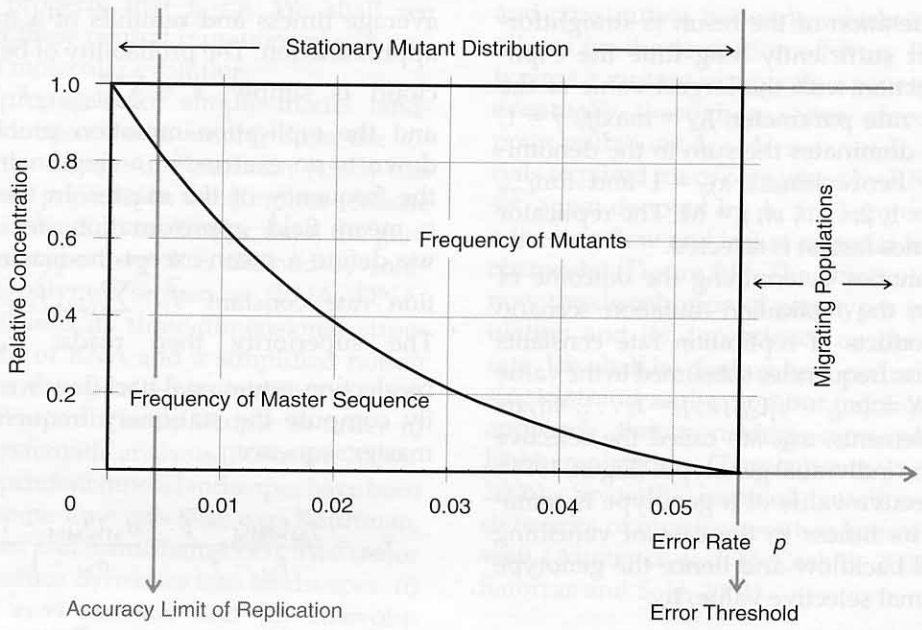

FIGURE 1.13 The genotypic error threshold. The fraction of mutants in stationary populations increases with the error rate p. The formation of a stable stationary mutant distributions, the quasispecies, requires sufficient accuracy of replication: The error rate p has to be below a maximal value known as error threshold, $p < p_{max}$, tantamount to a minimal replication accuracy, $q > q_{min}$. Above threshold, populations migrate through sequence space in random walk-like manner (Huynen *et al.*, 1996; Fontana and Schuster, 1998a). There is also a lower limit to replication accuracy which is given by the maximum accuracy of the replication machinery.

Exact Solution of the Quasispecies Equation

Exact solutions of the kinetic equation (33) can be obtained by different techniques (Thompson and McBride, 1974; Jones *et al.*, 1976; Baake and Wagner, 2001; Saakian and Hu, 2006). A straightforward approach starts with a transformation of variables

$$z_k(t) = x_k(t) \cdot \exp\left(\int_0^t \phi(\tau)d\tau\right),$$

that leads to a linear first order differential equation, $\dot{\mathbf{z}} = \mathrm{W} \cdot \mathbf{z}$, which can be solved in terms of the eigenvalue problem

$$\mathrm{W} \cdot \zeta_k = \lambda_k \cdot \zeta_k \text{ with } \zeta_k = \sum_{j=1}^{m} h_{kj} z_j \text{ and}$$
$$\Lambda = \mathrm{H} \cdot \mathrm{W} \cdot \mathrm{H}^{-1}.$$

The eigenvectors ζ_k are linear combinations of the variables z and represent the normal modes of the replication-mutation network, $\Lambda = \{\lambda_1, \lambda_2, \ldots, \lambda_m\}$ is a diagonal matrix, and the transformation matrix $\mathbf{H}$ contains the coefficients for the eigenvectors. The replication–mutation equation written in terms of eigenvectors of W is of the simple form: $\dot{\zeta}_k = \lambda_k \cdot \zeta_k$ and the solutions after re-introduction of constant population size through the constraint $\phi(t)$ are the same as in equation (33b).

In cases where all genotypes have non-zero fitness and $\mathbf{Q}$ is a primitive matrix,[9] Perron–Frobenius theorem (Seneta, 1981) applies: The largest eigenvalue λ_0 is real, positive, and non-degenerate.[10] The eigenvector ζ_0

[9] A square matrix $\mathbf{A}$ with non-negative entries is a primitive matrix, if and only if there exists a positive integer k such that A^k has only strictly positive entries.

[10] A non-degenerate eigenvalue has only one unique eigenvector. Twofold degeneracy, for example, means that two eigenvectors are associated with the eigenvalue and all linear combinations of the two eigenvectors are also solutions of the eigenvalue problem associated with the (twofold) degenerate eigenvalue.

belonging to the largest eigenvalue λ_0 is therefore unique, in addition it has strictly positive components. This purely mathematical result has important implications for the replication–mutation system:

(i) Since $\lambda_0 > \lambda_k \forall\ k = 1, 2, \ldots, m-1$ the eigenvector ζ_0 outgrows all other eigenvectors ζ_k and determines the distribution of genotypes in the population after sufficiently long time: ζ_0 is the stationary distribution of genotypes called the quasispecies.

(ii) All genotypes of the population, $\{\mathbf{I}_1, \mathbf{I}_2, \ldots, \mathbf{I}_m\}$ are present in the quasispecies although the concentration may be extremely small.

It is important to note that quasispecies can also exist in cases where the Perron–Frobenius theorem is not fulfilled. As an example we consider an extreme case of lethal mutants: Only genotype $\mathbf{I}_1$ has a positive fitness value, $f_1 > 0$ and $f_2 = \ldots = f_m = 0$, only the entries $w_{k1} = f_1 Q_{k1}$ are non-zero and hence

$$W = \begin{pmatrix} w_{11} & 0 & \ldots & 0 \\ w_{21} & 0 & \ldots & 0 \\ \vdots & \vdots & \ddots & \vdots \\ w_{m1} & 0 & \ldots & 0 \end{pmatrix} \quad \text{and}$$

$$W^k = w_{11}^k \begin{pmatrix} 1 & 0 & \ldots & 0 \\ \frac{w_{21}}{w_{11}} & 0 & \ldots & 0 \\ \vdots & \vdots & \ddots & \vdots \\ \frac{w_{m1}}{w_{11}} & 0 & \ldots & 0 \end{pmatrix}$$

Clearly, W is not primitive in this example, but $\bar{\mathbf{x}} = (Q_{11}, Q_{21}, \ldots, Q_{m1})$ is a stable stationary mutant distribution and for $Q_{11} > Q_{j1}$ $j = 2, \ldots, m$ (correct replication occurs more frequently than a particular mutation) genotype $\mathbf{I}_1$ is the master sequence. On the basis of a rather idiosyncratic mutation model consisting of a one-dimensional chain of mutations Wagner and Krall (1993) raised the claim that no error thresholds can occur in presence of lethal mutants. In a recent paper Takeuchi and Hogeweg (2007) used a realistic highdimensional mutation model and presented numerically computed examples of perfect error thresholds in the presence of lethal mutants.

Several authors (Leuthäusser, 1987; Tarazona, 1992; Franz *et al.*, 1993; Franz and Peliti, 1997) pointed out an equivalence between the quasispecies model and spin systems. Applying methods of statistical mechanics Franz and Peliti (1997) were able to show that for both models, the single peak fitness landscape and a random fitness model the error threshold corresponds to a first order phase transition. Valandro *et al.* (2000) demonstrated an isomorphism between the quasispecies and percolation models. Earlier work by Haken showed an analogy between selection of laser modes and quasispecies (Haken, 1983a, 1983b).

It is important to note that the appearance of a sharp error threshold depends on the distribution of fitness values in genotype space. The single-peak fitness landscape (Swetina and Schuster, 1982; Franz and Peliti, 1997), the multiple-peak fitness landscape (Saakian *et al.*, 2006), the random fitness landscape (Franz and Peliti, 1997; Campos, 2002), and realistic rugged landscapes (see below) give rise to sharp transitions whereas artificially smooth landscapes, which are often used in population genetics (Wiehe, 1997; Baake and Wagner, 2001), lead to gradual transitions from the replication–mutation ordered quasispecies to the uniform distribution of genotypes.

Random Drift and Truncation of Quasispecies

In contrast to the no-mutational-backflow approximation (35) the concentration of the master sequence does not drop to zero but converges to some small value beyond the error threshold. Nevertheless, the stationary solution of equation (33) changes abruptly within a narrow range of the error rate p. The cause of this change is an avoided crossing of the first two eigenvalues around $p_{\max}$ (Nowak and Schuster, 1989):[11] Below threshold the

[11] The notion of avoided crossing is used in quantum physics for a situation in which two eigenvalues that are coupled by a small off-diagonal element do not cross but approach each other very closely (Figure 1.14).

ζ_0 representing the quasispecies is associated with λ_0 the largest eigenvalue. Above threshold the previous eigenvector ζ_1 is associated with the largest eigenvalue. With further increasing error rates, p, this eigenvector approaches the uniform distribution of genotypes. A uniform distribution of genotypes, however, is no realistic object: Population sizes are almost always below 10^{15} molecules, a value that can be achieved in evolution experiments with molecules. The numbers of viruses in a host hardly exceed 10^{12}. The numbers of possible genotypes exceed these numbers by many orders of magnitude. There are, for example, about 6×10^{45} genotypes of tRNA sequence length $n = 76$. All the matter in the universe would not be sufficient to produce a uniform distribution of these molecules and, accordingly, no stationary distribution of sequences can be formed. Instead, the population drifts randomly through sequence space. This implies that all genotypes have only finite life times, inheritance breaks down and evolution becomes impossible unless there is a high degree of neutrality that can counteract this drastic imbalance (see below).

A similar situation occurs with rare mutations within individual quasispecies. Since every genotype can be reached from any other genotype by a sequel of individual mutations, all genotypes are present in the quasispecies no matter how small their concentrations might be. This, again is contradicting the discreteness at the molecular level. The solution of the problem distinguishes two classes of mutants: (i) frequent mutants, which are almost always present in realistic quasispecies, and (ii) rare mutants that are stochastic elements at the periphery of the deterministic mutant cloud.

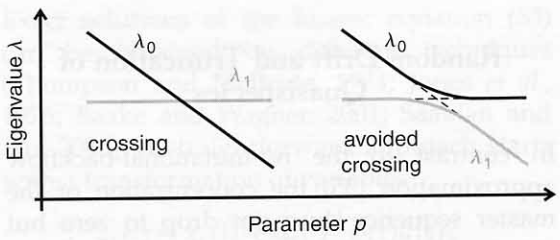

FIGURE 1.14 Avoided crossing of eigenvalues. Two eigenvalues, λ_0 and λ_1 cross as a function of the parameter under consideration (left hand side of the sketch). The two eigenvectors ζ_0 and ζ_1 are associated over the whole parameter range with λ_0 and λ_1, respectively. In avoided crossing (right hand side of the sketch) the eigenvalues do not cross, λ_0 and λ_1 are the largest and the largest but one over the whole range. The two eigenvectors, however, behave roughly as in case of crossing. Before the avoided crossing zone ζ_0 is associated with λ_0 and ζ_1 with λ_1, after crossing, the assignment is inverse: ζ_0 is associated with λ_1 and ζ_1 with λ_0.

In order to be able to study stochastic features of population dynamics around the error threshold in rigorous terms, the replication–mutation system was modeled by a multitype branching process (Demetrius *et al.*, 1985). The main result of this study is the derivation of an expression for the probability of survival to infinite time for the master sequence and its mutants. In the regime of sufficiently accurate replication, i.e. in the quasispecies regime, the survival probability is non-zero and decreases with increasing error rate p. At the critical accuracy pmax this probability becomes zero. This implies that all molecular species which are currently in the populations, master and mutants, will die out in finite times and new variants will appear. This scenario is tantamount to migration of the population through sequence space (Huynen *et al.*, 1996; Huynen, 1996). The critical accuracy $q_{\min}$, commonly seen as an error threshold for replication, can as well be understood as the localization threshold of the population in sequence space (McCaskill, 1984). Later investigations aimed directly at a derivation of the error threshold in finite populations (Nowak and Schuster, 1989; Alves and Fontanari, 1998).

Error Thresholds in Reality

Variations in the accuracy of *in vitro* replication can indeed be easily achieved because error rates can be tuned over many orders of magnitude (Leung *et al.*, 1989; Martinez *et al.*, 1994). The range of replication accuracies which are suitable for evolution is limited by the maximal accuracy that can be achieved by

the replication machinery and the minimum accuracy determined by the error threshold (Figure 1.13). Populations in constant environments have an advantage when they operate near the maximal accuracy because then they lose as few copies through mutation as possible. In highly variable environments the opposite is true: It pays to produce as many mutants as possible to maximize the chance of coping successfully with change. RNA viruses live in very variable environments since they have to cope with the highly effective defense mechanisms of the host cells.

The key parameter in testing error thresholds in real populations is the rate of spontaneous mutation, p. The experimental determination of mutation rates per replication and site, which is different from the observed frequency of mutations, is tricky mainly for two reasons: (i) deleterious and most neutral mutations will not be observed on the population level, because they are eliminated earlier by selection, and (ii) in the case of virus replication more than one replication take place in the infected cell (Drake, 1993; Drake and Holland, 1999). Careful evaluated results reveal a rate of roughly $\mu_g = 0.76$ per genome and replication, although the genome lengths vary from $n = 4200$ to $n = 13600$. This finding implies that the mutation rate per replication and nucleotide site is adjusted to the chain length. For a given error rate p the minimum accuracy of replication can be transformed into a maximum chain length $n_{\max}$.[12] Then the condition for the quasispecies error threshold provides a limit for the lengths of genotypes:

$$n < n_{\max} = -\frac{\ln \sigma}{\ln q} \approx \frac{\ln \sigma}{1-q} = \frac{\ln \sigma}{p}. \qquad (37)$$

RNA viruses mutate much more frequently than all other known organisms and this is presumably the consequence of two factors: (i) the defense mechanisms of the host provide a highly variable environment, which requires fast adaptation, and (ii) the small genome size is prohibitive for coding enzymes that replicate with high accuracy. The high mutation rate and the vast sequence heterogeneity of RNA viruses (Domingo *et al.*, 1998) suggest that most RNA viruses live indeed near the above mentioned critical value of replication accuracy (Domingo, 1996; Domingo and Holland, 1997) in good agreement with the relation between chain length n and error rate p mentioned above. For a review on medical application of the error threshold in antiviral therapies see, for example, Domingo and Holland (1997), Eigen (2002), Anderson *et al.* (2004), and the special issue of *Virus Research* (Domingo, ed., 2005). In a recent paper, Bull *et al.* (2007) present a theory of lethal mutagenesis that distinguishes crossing the error threshold from the decline of the population, $\lim c(t) \to 0$, which by construction cannot be seen in the quasispecies equation (33). The experimental verification of which of the two effects is the cause of lethal mutagenesis, however, seems to be very subtle.

The justification of the quasispecies concept in the description of RNA virus evolution has been challenged by Edward Holmes and co-workers (Jenkins *et al.*, 2001; Holmes and Moya, 2002; Comas *et al.*, 2005) (see also the reply by Domingo, 2002). They propagate the application of conventional population genetics to RNA virus evolution (Moya *et al.*, 2000, 2004) and raised several arguments against the application of the quasispecies concept to RNA virus evolution. Wilke (2005) performed a careful analysis of both approaches by means of thoughtfully chosen examples and showed the equivalence of both models that apparently has escaped the attention of the quasispecies opponents.[13] Indeed, it is only a matter

[12] The accuracy of replication is determined by the RNA replicase. Fine-tuning of the enzyme allows for an adjustment of the error rate within certain limits.

[13] On the basis of the paper by Wagner and Krall (1993), Wilke concluded erroneously that an error threshold cannot occur in the presence of lethal mutants. Wagner's result was an artifact of the assumption of an unrealistic one-dimensional sequence space. Takeuchi and Hogeweg (2007) have shown the existence of error thresholds on landscapes with lethal variants.

of model economy and taste whether one prefers the top-down approach of population genetics with the plethora of often unclear effects or the sometimes deeply confusing molecular bottom-up approach of biochemical kinetics with the enormous wealth of detail. To address issues of conventional evolutionary biology the language of population genetics provides an advantage; molecular biology and its results, however, are much more easily translated into the formalism of biochemical kinetics as the fast development of systems biology shows (Klipp *et al.*, 2005; Palsson, 2006).

Finally, we relate the concept of error threshold to the evolution of small prebiotic replicons. Uncatalyzed template-induced RNA replication can hardly be more accurate than $q = 0.99$ and this implies that the chain lengths of correctly replicated polynucleotides are limited to molecules with $n < 100$. RNA molecules of this size are neither in a position to code for efficiently replicating ribozymes nor can they develop a genetic code that allows for the evolution of protein enzymes. A solution for this dilemma, often called the Eigen paradox, was seen in functional coupling of replicons in the form of hypercycle (Eigen and Schuster, 1978a, 1978b).

EVOLUTION OF PHENOTYPES AND COMPUTER SIMULATION

The quasispecies concept discussed so far is unable to handle cases where many molecular species have the same maximal fitness.[14] In this section we deal with this case of neutrality first introduced by Kimura (1983) in order to interpret the data of molecular phylogenies. If we had only neutral genotypes the superiority of the master sequence becomes $\sigma_M = 1$ and the localization threshold of the quasispecies converges to the limit of absolute replication accuracy, $q_{min} = 1$. Clearly, the deterministic model fails, and we have to modify the kinetic equations. For example, there is ample evidence that RNA structures are precisely conserved despite vast sequence variation. Neutrality of RNA sequences with respect to secondary structure is particularly widespread and has been investigated in great detail (Fontana *et al.*, 1993; Schuster *et al.*, 1994; Reidys *et al.*, 1997; Reidys and Stadler, 2001). Here we sketch an approach to handle neutrality within the quasispecies approach (Reidys *et al.*, 2001) and then present computer simulations for a stochastic model based on the quasispecies equations (33) (Fontana and Schuster, 1987, 1998a, 1998b; Fontana *et al.*, 1989; Schuster, 2003).

A Model for Phenotype Evolution

Genotypes are ordered with respect to non-increasing selective values. The first k_1 different genotypes have maximal selective value: $w_1 = w_2 = \ldots = w_{k_1} = w_{max} = \tilde{w}_1$ (where $\sim$ indicates properties of groups of neutral phenotypes). The second group of neutral genotypes has the highest but one selective value: $w_{k1+1} = w_{k1+2} = \ldots = w_{k1+k2} = \tilde{w}_2 < \tilde{w}_1$, etc. Replication rate constants are assigned in the same way: $f_1 = f_2 = \ldots = f_{k1} = \tilde{f}_1$, etc. In addition, we define new variables, y_j ($j = 1, \ldots, \ell$), that lump together all genotypes folding into the same phenotype:

$$y_j = \sum_{i=k_{j-1}+1}^{k_j} x_i \text{ with } \sum_{j=1}^{\ell} y_j = \sum_{i=1}^{m} x_i = 1. \quad (38)$$

The phenotype with maximal fitness, the master phenotype, is denoted by "M." Since we are heading again for a kind of zeroth-order solution, we consider only the master phenotype and put $k_1 = k$. With $y_M = \sum_{i=1}^{k} x_i$ we obtain the following kinetic differential equation for the set of sequences forming the neutral network of the master phenotype:

$$\dot{y}_M = \sum_{i=1}^{k} \dot{x}_i = y_M(\tilde{f}_M Q_{kk} - \bar{E}) + \sum_{i=1}^{k}\sum_{j\neq i} f_j Q_{ji} x_j. \quad (39)$$

[14] Different examples of fitness landscapes with two highest peaks were analyzed and discussed by Schuster and Swetina (1988). This approach, however, cannot be extended to a substantially larger number of master genotypes.

The mean excess productivity of the population is, of course, independent of the choice of variables: $\bar{E} = \sum_{j=1}^{\ell} \tilde{f}_j y_j = \sum_{i=1}^{m} f_i x_i$.

The mutational backflow is split into two contributions, (i) mutational backflow on the neutral network and (ii) mutational backflow from genotypes not on the network.

$$\dot{y}_M = (\tilde{f}_M \tilde{Q}_{MM} - \bar{E}) y_M + \text{mutational backflow} \quad (40)$$

The next task is to compute the effective replication accuracy $\tilde{Q}_{MM}$.

Phenotypic Error Thresholds

An assumption for the distribution of neutral genotypes in sequence space is required for the calculation of the effective replication accuracy $\tilde{Q}_{MM}$ of the master phenotype. Two assumptions were made (i) uniform distribution of neutral sequences (Reidys *et al.*, 2001) and (ii) a binomial distribution for neutral substitutions as a function of the Hamming distance from the reference sequence (Takeuchi *et al.*, 2005). Both assumptions lead to an expression of the form

$$\tilde{Q}_{MM} = Q_{MM} + \Lambda(1 - Q_{MM}) = q^n \cdot F(q, \lambda, n)$$

where Λ is the fraction of neutral mutants in sequence space and λ is the degree of neutrality, the fraction of neutral mutants in the one-error neighborhood of the reference sequence. The functions $F(q, \lambda, n)$ are of the form

$$F^{(i)}(q, \lambda, n) = 1 + \lambda \frac{1 - q^n}{q^n} \text{ for assumption (i) and}$$

$$F^{(ii)}(q, \lambda, n) = \left(1 + \lambda \frac{1 - q}{q}\right)^n \text{ for assumption (ii).}$$

The second function was also used in a different version with a tunable parameter ν instead of λ (Wilke, 2001). The calculation of expressions for phenotypic error thresholds is now straight-forward and leads to the following two expressions for the minimal replication accuracy q_{min}:

$$q_{min}^{(i)} = (1 - p_{max}^{(i)}) = \left(\frac{\sigma_M^{-1} - \lambda_M}{1 - \lambda_M}\right)^{1/n} \text{ and} \quad (41)$$

$$q_{min}^{(ii)} = (1 - p_{max}^{(ii)}) = \frac{\sigma_M^{-1/n} - \lambda_M}{1 - \lambda_M} \quad (42)$$

Both equations converge to the expression for genotypic error threshold (36) in the limit $\lambda \to 0$. Both approaches predict a decrease of the minimum accuracy with increasing neutrality but the assumption (ii) leads to a much smaller effect that becomes dominant only close to complete neutrality $\lambda \to 1$. The conclusion of Takeuchi *et al.* (2005) is therefore that neutrality has a very limited influence on the minimum replication accuracy.

Between the genotypic and the phenotypic error threshold the population migrates in sequence space but the phenotype is still conserved. Precisely this behavior is postulated in the observed phylogenies of RNA molecules and RNA viruses. Because of the deterministic nature of the quasispecies equation (33) random drift on neutral spaces or subspaces cannot be described. Such a behavior, however, can be directly observed and analyzed in computer simulations of RNA evolution, which will be the subject of the next subsection.

Computer Simulations

The concept of the phenotypic error threshold allows for an extension of the kinetic equations to the regime of random drift without, however, providing insights into the stochastic process itself. Since a sufficiently high degree of neutrality is required to observe random drift, the RNA sequence-structure map was chosen for the computer simulations because it was known to give rise to vast neutrality and to support random drift (Fontana *et al.*, 1993; Schuster *et al.*, 1994; Huynen *et al.*, 1996). The flow reactor shown in Figure 1.9 was chosen as a proper chemical environment for the simulation of RNA evolution (Fontana

and Schuster, 1998a, 1998b). We present only the result that is relevant here (for more details see Schuster, 2003). Solutions of the master equation (Gardiner, 2004) corresponding to the reaction network of the quasispecies equation (33) are approximated by sampling numerically computed trajectories according to a procedure proposed by Gillespie (1976, 1977a, 1977b). In order to be able to evaluate the progress in the individual simulations a fixed target that happens to be the secondary structure of $tRNA^{phe}$, S_τ, was chosen. The fitness function, $f_k = (\alpha + d_S(S_k, S_\tau)/n)^{-1}$, increases with decreasing distance to the target structure S_τ.[15] The trajectories end after the target structure has been reached. Thus the stochastic process has two absorbing barriers: (i) extinction of the population and (ii) reaching the target. The question is whether or not the populations become extinct and whether the trajectories of surviving populations reach the target in reasonable or astronomic times.

A typical trajectory is shown in Figure 1.15. The stochastic process occurs on two timescales: (i) fast adaptive phases during which the population approaches the target are interrupted by (ii) slow epochs of random drift at constant distance from the target, and this gives trajectories the typical stepwise appearance. At the beginning of an adaptive phase the genotype distribution in sequence space is very narrow, typical are widths below Hamming distance 5 for population sizes of $N = 3000$. Then, along the plateau, the width of the population increases substantially up to values of 30 in Hamming distance. At first the population broadens but still occupies a coherent region in sequence space, later it is split into individual clones that continue to diverge in sequence space.[16] Interestingly, the consensus sequence of the population tantamount to the position of the population center in sequence space stays almost invariant during the quasistationary epochs. Eventually, the spreading population finds a genotype of higher fitness and a new adaptive phase is initiated. This is mirrored in sequence space by a jump of the population center and a dramatic narrowing of the population width. In other words, the beginning of a new adaptive period represents a bottleneck in sequence space through which the population has to pass in order to continue the adaptation process. Thus the evolutionary process is characterized by a succession of optimization periods in sequence space, where quasispecies-like behavior is observed, and random drift epochs, during which the population spreads until it finds a genotype that is suitable for further optimization. Two types of processes were observed in the random drift domain: (i) changing RNA sequences at conservation of the secondary structure and (ii) changing sequences overlaid by a random walk in the subspace of structures with equal distance to target. Population sizes were varied between $N = 100$ and $N = 100\,000$ but no significant change was observed in the qualitative behavior of the system except the trivial effect that larger populations can cover greater areas in sequence space.

Systematic studies on the parameter dependence of RNA evolution were reported in a recent simulation (Kupczok and Dittrich, 2006). Increase in mutation rate leads to an error threshold phenomenon that is close to one observed with quasispecies on a single-peak landscape as described above (Swetina and Schuster, 1982; Eigen *et al.*, 1989). Evolutionary optimization becomes more efficient[17] with increasing error rate until the error threshold is reached. Further increase in the error rate leads to an abrupt breakdown of the optimization process. As expected, the distribution of replication rates or fitness values f_k in sequence space is highly relevant too: steep

[15] For the definition of a distance between two structures, $d_S(S_k, S_j)$, see the footnote of Table 1.1.

[16] The same phenomenon has been observed in the evolution of populations on flat landscapes (Derrida and Peliti, 1991).

[17] Efficiency of evolutionary optimization is measured by average and best fitness values obtained in populations after a predefined number of generations.

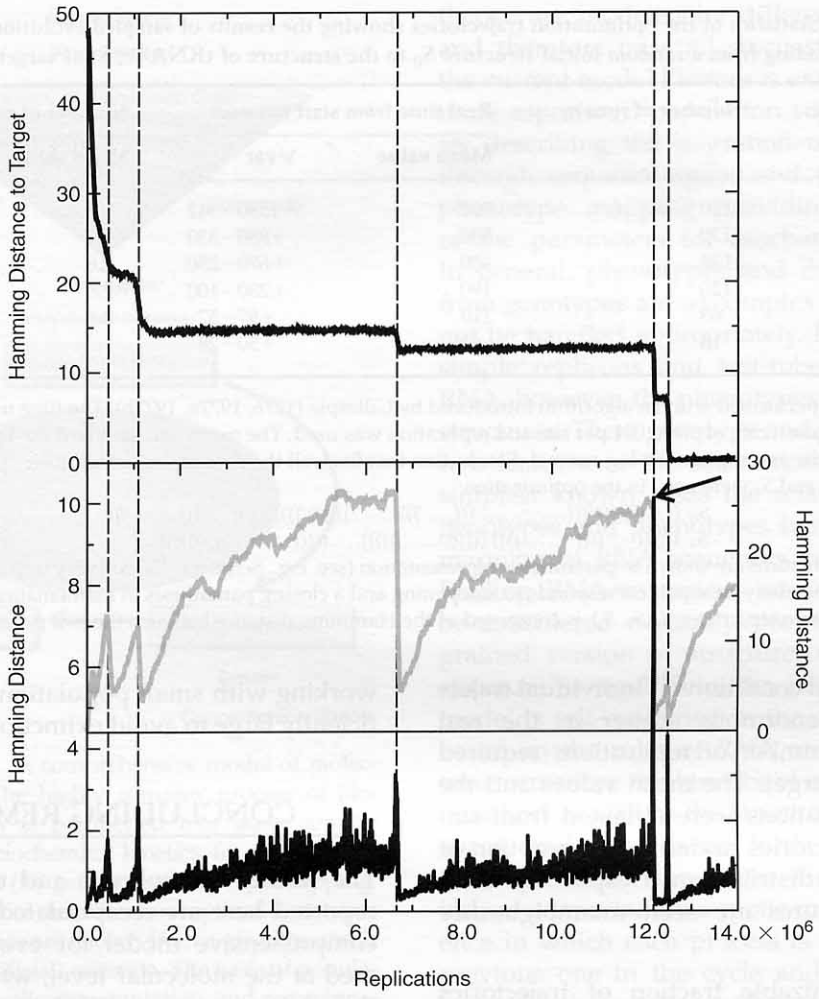

Figure 1.15 Evolutionary optimization of RNA structure. Shown is a single trajectory of a simulation of RNA optimization towards a $tRNA^{phe}$ target with population size $N = 3000$, the fitness function $f_k = (\alpha + d_S(S_k, S_\tau)/n)^{-1}$ with $\alpha = 0.01$ and $n = 76$, and mutation rate $p = 0.001$ per site and replication. The figure shows as functions of time: (i) the distance to target averaged over the whole population, $d_S(S_i, S_\tau)(t)$ (upper black curve), (ii) the mean Hamming distance within the population, $d_P(t)$ (gray, right ordinate), and (iii) the mean Hamming distance between the populations at time t and $t + \Delta t$, $d_C(t, \Delta t)$ (lower black curve) with a time increment of $\Delta t = 8000$. The end of plateaus (vertical lines) are characterized by a collapse in the width of the population and a peak in the migration velocity corresponding to a bottleneck in diversity and a jump in sequence space. The arrow indicates a remarkably sharp peak of Hamming distance 10 at the end of the second long plateau ($t \approx 12.2 \times 10^6$ replications). On the plateaus the center of the cloud stays practically constant (the speed of migration is Hamming distance 0.125 per 1000 replications) corresponding to a constant consensus sequence. Each adaptive phase is preceded by a drastic reduction in genetic diversity, $d_P(t)$, then the diversity increases during the quasistationary epochs and reaches a width of Hamming distance more than 25 on long plateaus.

and rugged fitness functions lead to the sharp threshold behavior as observed with single-peak landscapes, whereas smooth and flat landscapes give rise to a broad maximum of optimization efficiency without an indication of a threshold-like behavior.

Table 1.1 collects some numerical data obtained from repeated evolutionary trajectories

TABLE 1.1 Statistics of the optimization trajectories showing the results of sampled evolutionary trajectories leading from a random initial structure S_0 to the structure of $tRNA^{phe}$, $S\tau$ as target.[a]

Population size N	Number of runs n_t	Real time from start to target		Number of replications (10^7)	
		Mean value	$\sqrt{\text{var}}$	Mean value	$\sqrt{\text{var}}$
1000	120	900	+1380−542	1.2	+3.1−0.9
2000	120	530	+880−330	1.4	+3.6−1.0
3000	1199	400	+670−250	1.6	+4.4−1.2
10000	120	190	+230−100	2.3	+5.3−1.6
30000	63	110	+97−52	3.6	+6.7−2.3
100000	18	62	+50−28	–	–

Simulations were performed with an algorithm introduced by Gillespie (1976, 1977a, 1977b). The time unit is here undefined. A mutation rate of $p = 0.001$ per site and replication was used. The mean and standard deviation were calculated under the assumption if a log-normal distribution that fits well the data of the simulations.

[a]The structures S_0 and S_τ were used in the optimization:

S_0: ((·(((((((((((((..... (((....)))....))))))·))))))·)) ... (((.....)))

S_τ: ((((((... ((((.....)))))·(((((.....)))))…..(((((.....)))))·))))))….

The secondary structures are shown in parentheses representation (see, e.g., Schuster, 2006). Every unpaired nucleotide is denoted by a dot, every base pair corresponds to an opening and a closing parenthesis in mathematical notation. The distance between two structures, $d_S(S_k, S_j)$, is computed as the Hamming distance between the two parentheses notation.

under identical conditions.[18] Individual trajectories show enormous scatter in the real time or the number of replications required to reach the target. The mean values and the standard deviations were obtained from statistics of trajectories under the assumption of a log-normal distribution. Despite the scatter three features are seen unambiguously detectable:

(i) A recognizable fraction of trajectories leads to extinction only at very small population sizes, $N < 25$. In larger populations the target is reached with probabilities of measure 1.

(ii) The time to target decreases with increasing population size.

(iii) The number of replications required to reach target increases with population size.

Combining items (ii) and (iii) allows for a clear conclusion concerning time and material requirements of the optimization process: Fast optimization requires large populations whereas economic use of material suggests working with small population sizes just sufficiently large to avoid extinction.

[18] Identical means here that everything was kept constant except the seeds for the random number generators.

CONCLUDING REMARKS

The results on replicons and their evolution reported here are recapitulated in terms of a comprehensive model for evolution considered at the molecular level, which was introduced ten years ago (Schuster, 1997a, 1997b). In most previous models phenotypes were considered only in terms of parameters contained in the kinetic equations and therefore an attempt to include phenotypes as integral parts of the model was made. Mutation and recombination act on genotypes whereas the target of selection, the fitness, is a property of phenotypes. The relations between genotypes and phenotypes are thus an intrinsic part of evolution and no theory can be complete without considering them. The complex process of evolution is partitioned into three simpler phenomena (Figure 1.16): (i) biochemical kinetics, (ii) migration of populations, and (iii) genotype–phenotype mapping. Conventional biochemical kinetics as well as replicator dynamics including quasispecies

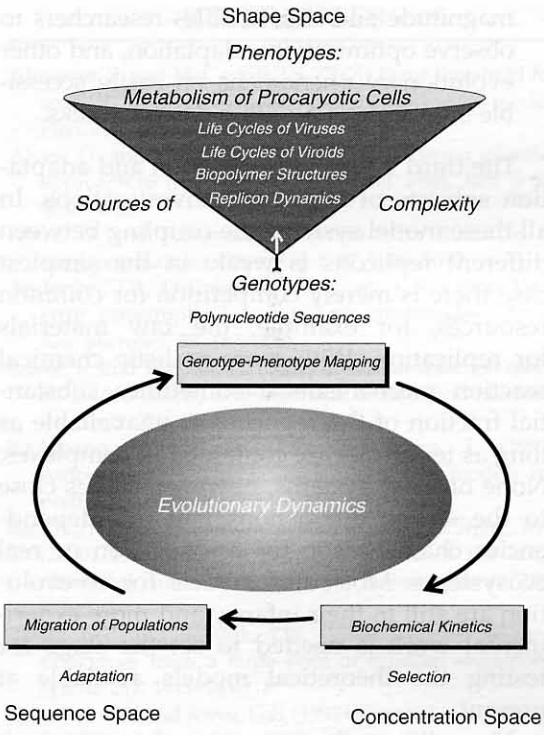

FIGURE 1.16 A comprehensive model of molecular evolution. The highly complex process of biological evolution is partitioned into three simpler phenomena: (i) biochemical kinetics, (ii) migration of populations, and (iii) genotype–phenotype mapping. Biochemical kinetics describes how optimal genotypes with optimal genes are chosen from a given reservoir by natural (or artificial) selection. The basis of population genetics is replication, mutation, and recombination mostly modeled by kinetic differential equations. In essence, kinetics is concerned with selection and other evolutionary phenomena occurring on short time-scales. Population support dynamics describes how the genetic reservoirs change when populations migrate in the huge space of all possible genotypes. Issues are the internal structure of populations and the mechanisms by which the regions of high fitness are found in sequence or genotype space. Support dynamics is dealing with the long-time phenomena of evolution, for example, with optimization and adaptation to changes in the environment. Genotype–phenotype mapping represents a core problem of evolutionary thinking since the dichotomy between genotypes and phenotypes is the basis of Darwin's principle of variation and selection: Variations and their results are uncorrelated in the sense that a mutation yielding a fitter phenotype does not occur more frequently because of the increase in fitness.

theory are modeled by differential equation and therefore miss all stochastic aspects. In the current model kinetics is extended by two more aspects: (i) population support dynamics describing the migration of populations through sequence space and (ii) genotype–phenotype mapping providing the source of the parameters for biochemical kinetics. In general, phenotypes and their formation from genotypes are so complex that they cannot be handled appropriately. In reactions of simple replicons and test-tube evolution of RNA, however, the phenotypes are molecular structures. Then, genotype and phenotype are two features of the same molecule. In these simplest known cases the relations between genotypes and phenotypes boil down to the mapping of RNA sequences onto structures. Folding RNA sequences into structures can be considered explicitly provided a coarse-grained version of structure, the secondary structure, is used (Schuster, 2006). This RNA model is self-contained in the sense that it is based on the rules of RNA secondary structure formation, the kinetics of replication and mutation as well as the structure of sequence space, and it needs no further inputs. The three processes shown in Figure 1.16 are indeed connected by a cyclic mutual dependence in which each process is driven by the previous one in the cycle and provides the input for the next one: (i) folding sequences into structures yields the input for biochemical kinetics, (ii) biochemical kinetics describes the arrival of new genotypes through mutation and the disappearance of old ones through selection, and determines thereby how and where the population migrates, and (iii) migration of the population in sequence space eventually creates the new genotypes that are to be mapped into phenotypes thereby completing the cycle. The model of evolutionary dynamics has been applied to interpret the experimental data on molecular evolution and it was implemented for computer simulations of neutral evolution and RNA optimization in the flow reactor (Huynen *et al.*, 1996; Fontana and Schuster, 1998a, 1998b). Computer simulations allow to follow the

optimization process at the molecular level in full detail. What is still needed is a comprehensive mathematical description combining the three processes.

The work with RNA replicons has had a pioneering character. Both the experimental approach to evolution in the laboratory and the development of a theory of evolution are much simpler for RNA than in case of proteins or viruses. On the other hand, genotype and phenotype are more closely linked in RNA than in any other system. The next logical step in theory and experiment consists of the development of a coupled RNA–protein system that makes use of both replication and translation. This achieves the effective decoupling of genotype and phenotype that is characteristic for all living organisms: RNA is the genotype, protein the phenotype and thus, genotype and phenotype are no longer housed in the same molecule. The development of a theory of evolution in the RNA–protein world requires, in addition, an understanding of the notoriously difficult sequence–structure relations in proteins. Issues that are becoming an integral part of research on early replicons are (i) primitive forms of metabolism that can provide the material required for replication (and translation) and (ii) spatial isolation in vesicles or some amphiphilic material that forms compartments.

Molecular evolution experiments with RNA molecules and the accompanying theoretical descriptions made three important contributions to evolutionary biology:

1. The role of replicative units in the evolutionary process has been clarified, the conditions for the occurrence of error thresholds have been laid down, and the role of neutrality has been elucidated.
2. The Darwinian principle of (natural) selection has shown to be no privilege of cellular life, since it is valid also in serial transfer experiments, flow-reactors, and other laboratory assays such as SELEX.
3. Evolution in molecular systems is faster than organismic evolution by many orders of magnitude and thus enables researchers to observe optimization, adaptation, and other evolutionary phenomena on easily accessible time-scales, i.e. within days or weeks.

The third issue made selection and adaptation subjects of laboratory investigations. In all these model systems the coupling between different replicons is weak: in the simplest case there is merely competition for common resources, for example, the raw materials for replication. With more realistic chemical reaction mechanisms a sometimes substantial fraction of the replicons is unavailable as long as templates are contained in complexes. None of these systems, however, comes close to the strong interactions and interdependencies characteristic for co-evolution or real ecosystems. Molecular models for co-evolution are still in their infancy and more experimental work is needed to set the stage for testing the theoretical models available at present.

Virus life cycles represent the next logical step in increasing complexity of genotype–phenotype interactions. The pioneering paper by Weissmann (1974) has shown the way to proceed in the case of an RNA phage that is among the most simple candidates, and indeed the development of phages in bacterial cells can be modeled with sufficient accuracy. A lot of elegant work has been done since then and a wealth of data and models is available but many more experiments and more detailed theories are necessary to decipher the complex interactions of host–pathogen systems on the molecular level.

ACKNOWLEDGMENTS

The work reported here was supported financially by the Austrian Fonds zur Förderung der Wissenschaftlichen Forschung, (Projects No. 11065-CHE, 12591-INF, 13093-GEN, and 14898-MAT), by the European Commission (Project No.PL970189), and by the Santa Fe Institute.

REFERENCES

Altmeyer, S. and McCaskill, J.S. (2001) Error threshold for spatially resolved evolution in the quasispecies model. *Phys. Rev. Lett.* **86**, 5819–5822.

Alves, D. and Fontanari, J.F. (1996) Population genetics approach to the quasispecies model. *Phys. Rev. E* **54**, 4048–4053.

Alves, D. and Fontanari, J.F. (1998) Error threshold in finite populations. *Phys. Rev. E* **57**, 7008–7013.

Anderson, J.P., Daifuku, R. and Loeb, L.A. (2004) Viral error catastrophe by mutagenic nucleosides. *Annu. Rev. Microbiol.* **58**, 183–205.

Baake, E. and Wagner, H. (2001) Mutation-selection models solved exactly with methods of statistical mechanics. *Genet. Res. Camb.* **78**, 93–117.

Bachmann, P.A., Luisi, P.L. and Lang, J. (1992) Autocatalytic self-replicating micelles as models for prebiotic structures. *Nature* **357**, 57–59.

Ban, N., Nissen, P., Hansen, J., Moore, P.B. and Steitz, T.A. (2000) The complete atomic structure of the large ribosomal subunit at 2.4Å resolution. *Science* **289**, 905–920.

Bartel, D.P. and Szostak, J.W. (1993) Isolation of new ribozymes from a large pool of random sequences. *Science* **261**, 1411–1418.

Beaudry, A.A. and Joyce, G.F. (1992) Directed evolution of an RNA enzyme. *Science* **257**, 635–641.

Biebricher, C.K. and Eigen, M. (1988) Kinetics of RNA replication by Qβ replicase. In: *RNA Genetics. RNA Directed Virus Replication* (E. Domingo, J.J. Holland and P. Ahlquist, eds), Vol. I, pp. 1–21. Boca Raton, FL: CRC Press.

Brasier, M.D., Green, O.R., Jephcoat, A.B., Kleppe, A.K., Van Kranendonk, M.J., Lindsay, J.F. *et al.* (2002) Questioning the evidence for Earth's oldest fossils. *Nature* **416**, 76–81.

Breaker, R.R. and Joyce, G.F. (1994) Emergence of a replicating species from an *in vitro* RNA evolution reaction. *Proc. Natl Acad. Sci. USA* **91**, 6093–6097.

Bull, J.J., Sanjuán, R. and Wilke, C.O. (2007) Theory of lethal mutagensis for viruses. *J. Virol.* **81**, 2930–2939.

Campos, P.R.A. (2002) Error threshold transition in the random-energy model. *Phys. Rev. E* **66**, 062904.

Cate, J.H., Gooding, A.R., Podell, E., Zhou, K., Golden, B.L., Kundrot, C.E. *et al.* (1996) Crystal structure of a group I ribozyme domain: Principles of RNA packing. *Science* **273**, 1678–1685.

Cavalier-Smith, T. (2001) Obcells as proto-organisms: Membrane heredity, lithophosphorylation, and the origins of the genetic code, the first cells, and photosynthesis. *J. Mol. Evol.* **53**, 555–595.

Cech, T.R. (1983) RNA splicing: Three themes with variations. *Cell* **34**, 713–716.

Cech, T.R. (1986) RNA as an enzyme. *Sci. Am.* **255**, 76–84.

Cech, T.R. (1990) Self-splicing of group I introns. *Annu. Rev. Biochem.* **59**, 543–568.

Comas, I., Moya, A. and González-Candelas, F. (2005) Validating viral quasispecies with digital organisms: A re-examiniation of the critical mutation rate. *BMC Evol. Biol.* **5**, 1–10.

Cuenoud, B. and Szostak, J.W. (1995) A DNA metalloenzyme with DNA ligase activity. *Nature* **375**, 611–614.

Demetrius, L., Schuster, P. and Sigmund, K. (1985) Polynucleotide evolution and branching processes. *Bull. Math. Biol.* **47**, 239–262.

Derrida, B. and Peliti, L. (1991) Evolution in a flat fitness landscape. *Bull. Math. Biol.* **53**, 355–382.

Domingo, E. (1996) Biological significance of viral quasispecies. *Viral Hepatitis Rev.* **2**, 247–261.

Domingo, E. (2002) Quasispecies theory in virology. *J. Virol.* **76**, 463–465.

Domingo, E. (2005) Virus entry into error catastrophe as a new antiviral strategy. *Virus Res.* **107**, 115–228.

Domingo, E. and Holland, J.J. (1997) RNA virus mutations and fitness for survival. *Annu. Rev. Microbiol.* **51**, 151–178.

Domingo, E., Sabo, D., Taniguchi, T. and Weissmann, C. (1998) Nucleotide sequence heterogeneity of an RNA phage. *Cell* **13**, 735–744.

Drake, J.W. (1993) Rates of spontaneous mutation among RNA viruses. *Proc. Natl Acad. Sci. USA* **90**, 4171–4175.

Drake, J.W. and Holland, J.J. (1999) Mutation rates among RNA viruses. *Proc. Natl Acad. Sci. USA* **96**, 13910–13913.

Eigen, M. (1971) Selforganization of matter and the evolution of macromolecules. *Naturwissenschaften* **58**, 465–523.

Eigen, M. (2002) Error catastrophe and antiviral strategy. *Proc. Natl Acad. Sci. USA* **99**, 13374–13376.

Eigen, M. and Schuster, P. (1977) The hypercycle. A principle of natural self-organization. Part A: Emergence of the hypercycle. *Naturwissenschaften* **64**, 541–565.

Eigen, M. and Schuster, P. (1978a) The hypercycle. A principle of natural self-organization. Part B: The abstract hypercycle. *Naturwissenschaften* **65**, 7–41.

Eigen, M. and Schuster, P. (1978b) The hypercycle. A principle of natural self-organization. Part C: The realistic hypercycle. *Naturwissenschaften* **65**, 341–369.

Eigen, M. and Schuster, P. (1982) Stages of emerging life—Five principles of early organization. *J. Mol. Evol.* **19**, 47–61.

Eigen, M., McCaskill, J. and Schuster, P. (1989) The molecular quasispecies. *Adv. Chem. Phys.* **75**, 149–263.

Eigen, M., Biebricher, C.K., Gebinoga, M. and Gardiner, W.C., Jr. (1991) The hypercycle. Coupling of RNA and protein biosynthesis in the infection cycle of an RNA bacteriophage. *Biochemistry* **30**, 11005–11018.

Ekland, E.H. and Bartel, D.P. (1996) RNA-catalysed RNA polymerization 54 using nucleoside triphosphates. *Nature* **382**, 373–376.

Ekland, E.H., Szostak, J.W. and Bartel, D.P. (1995) Structurally complex and highly active RNA ligases derived from random RNA sequences. *Science* **269**, 364–370.

Eschenmoser, A. (1993) Hexose nucleic acids. *Pure Appl. Chem.* **65**, 1179–1188.

Fahy, E., Kwoh, D.Y. and Gingeras, T.R. (1991) Self-sustained sequence replication (3SR): An isothermal transcription-based amplification system alternative to PCR. *PCR Methods Appl.* **1**, 25–33.

Ferré-D'Amaré, A.R., Zhou, K. and Doudna, J.A. (1998) Crystal structure of a hepatitis delta virus ribozyme. *Nature* **395**, 567–574.

Fontana, W. and Schuster, P. (1987) A computer model of evolutionary optimization. *Biophys. Chem.* **26**, 123–147.

Fontana, W. and Schuster, P. (1998a) Continuity in evolution. On the nature of transitions. *Science* **280**, 1451–1455.

Fontana, W. and Schuster, P. (1998b) Shaping space. The possible and the attainable in RNA genotype-phenotype mapping. *J. Theor. Biol.* **194**, 491–515.

Fontana, W., Schnabl, W. and Schuster, P. (1989) Physical aspects of evolutionary optimization and adaptation. *Phys. Rev. A* **40**, 3301–3321.

Fontana, W., Konings, D.A.M., Stadler, P.F. and Schuster, P. (1993) Statistics of RNA secondary structures. *Biopolymers* **33**, 1389–1404.

Fox, S.W. and Dose, H. (1977) *Molecular Evolution and the Origin of Life.* New York: Academic Press.

Frank, F.C. (1953) On spontaneous asymmetric synthesis. *Biochim. Biophys. Acta* **11**, 459–463.

Franz, S. and Peliti, L. (1997) Error threshold in simple landscapes. *J. Phys. A: Math. Gen.* **30**, 4481–4487.

Franz, S., Peliti, L. and Sellitto, M. (1993) Error threshold in simple landscapes. *J. Phys. A: Math. Gen.* **26**, L1195–L1199.

Gánti, T. (1997) Biogenesis itself. *J. Theor. Biol.* **187**, 583–593.

Gardiner, C.W. (2004) *Handbook of Stochastic Methods for Physics, Chemistry and the Natural Sciences, Springer Series in Synergetics*, 3rd edn. Berlin: Springer-Verlag.

Gesteland, R.F. and Atkins, J.F. (eds) (1993). *The RNA World.* Plainview, NY: Cold Spring Harbor Laboratory Press.

Gesteland, R.F., Thomas, R.C. and Atkins, J.F. (2006). *The RNA World*, 3rd edn. Plainview, NY: Cold Spring Harbor Laboratory Press.

Gilbert, W. (1986) The RNA world. *Nature* **319**, 618.

Gillespie, D.T. (1976) A general method for numerically simulating the stochastic time evolution of coupled chemical reactions. *J. Comp. Phys.* **22**, 403–434.

Gillespie, D.T. (1977a) Concerning the validity of the stochastic approach to chemical kinetics. *J. Stat. Phys.* **16**, 311–318.

Gillespie, D.T. (1977b) Exact stochastic simulation of coupled chemical reactions. *J. Phys. Chem.* **81**, 2340–2361.

Green, R. and Noller, H.F. (1997) Ribosomes and translation. *Annu. Rev. Biochem.* **66**, 679–716.

Guerrier-Takada, C., Gardiner, K., Marsh, T., Pace, N. and Altman, S. (1983) The RNA moiety of ribonuclease P is the catalytic subunit of the enzyme. *Cell* **35**, 849–857.

Haken, H. (1983a) *Laser Theory.* New York: Springer-Verlag.

Haken, H. (1983b) *Synergetics. An Introduction. Springer Series in Synergetics*, 3rd edn. Berlin: Springer-Verlag.

Happel, R. and Stadler, P.F. (1999) Autocatalytic replication in a CSTR and constant organization. *J. Math. Biol.* **38**, 422–434.

Hofbauer, J. (1981) On the occurrence of limit cycles in the Volterra-Lotka differential equation. *Nonlin. Anal.* **5**, 1003–1007.

Hofbauer, J. and Sigmund, K. (1998) *Dynamical Systems and the Theory of Evolution.* Cambridge: Cambridge University Press.

Hofbauer, J., Schuster, P. and Sigmund, K. (1981) Competition and cooperation in catalytic selfreplication. *J. Math. Biol.* **11**, 155–168.

Holmes, E.C. and Moya, A. (2002) Is the quasispecies concept relevant to RNA viruses? *J. Virol.* **76**, 460–462.

Huynen, M.A. (1996) Exploring phenotype space through neutral evolution. *J. Mol. Evol.* **43**, 165–169.

Huynen, M.A., Stadler, P.F. and Fontana, W. (1996) Smoothness within ruggedness. The role of neutrality in adaptation. *Proc. Natl Acad. Sci. USA* **93**, 397–401.

Jenkins, G.M., Worobey, M., Woelk, C.H. and Holmes, E.C. (2001) Evidence for the non-quasispecies evolution of RNA viruses. *Mol. Biol. Evol.* **18**, 987–994.

Jenne, A. and Famulok, M. (1998) A novel ribozyme with ester transferase activity. *Chem. Biol.* **5**, 23–34.

Jiang, L., Suri, A.K., Fiala, R. and Patel, D.J. (1997) Saccharide-RNA recognition in an aminoglycoside antibiotic-RNA aptamer complex. *Chem. Biol.* **4**, 35–50.

Jones, B.L., Enns, R.H. and Rangnekar, S.S. (1976) On the theory of selection of coupled macromolecular systems. *Bull. Math. Biol.* **38**, 15–28.

Joyce, G.F. (1991) The rise and fall of the RNA world. *The New Biologist* **3**, 399–407.

Kauffman, S.A. (1993) *The Origins of Order. Self-Organization and Selection in Evolution.* New York: Oxford University Press.

Kimura, M. (1983) *The Neutral Theory of Molecular Evolution.* Cambridge: Cambridge University Press.

Klipp, E., Herwig, R., Kowald, A., Wieling, C. and Lehrach, H. (2005) *Systems Biology in Practice. Concepts, Implementation, and Application.* Weinheim: Wiley-VCH.

Klussmann, S. (ed.) (2006) The Aptamer Handbook. *Functional Oligonucleotides and Their Applications.* Weinheim: Wiley-VCH.

Kramer, F.R., Mills, D.R., Cole, P.E., Nishihara, T. and Spiegelman, S. (1974) Evolution in vitro: Sequence and phenotype of a mutant RNA resitant to ethidium bromide. *J. Mol. Biol.* **89**, 719–736.

Kupczok, A. and Dittrich, P. (2006) Determinants of simulated RNA evolution. *J. Theor. Biol.* **238**, 726–735.

Lee, D.H., Granja, J.R., Martinez, J.A., Severin, K. and Ghadiri, M.R. (1996) A self-replicating peptide. *Nature* **382**, 525–528.

Lee, D.H., Severin, K., Yokobayashi, Y. and Ghadiri, M.R. (1997) Emergence of symbiosis in peptide self-replication through a hypercyclic network. *Nature* **390**, 591–594.

Leung, D.W., Chen, E. and Goeddel, D.V. (1989) A method for random mutagenesis of a defined DNA segment

using a modified polymerase chain reaction. *Technique* **1**, 11–15.

Leuthäusser, I. (1987) Statistical mechanics of Eigen's evolution model. *J. Statist. Phys.* **48**, 343–360.

Levitan, B. and Kauffman, S.A. (1995) Adaptive walks with noisy fitness measurements. *Mol. Diversity* **1**, 53–68.

Li, T. and Nicolaou, K.C. (1994) Chemical self-replication of palindromic duplex DNA. *Nature* **369**, 218–221.

Lohse, P.A. and Szostak, J.W. (1996) Ribozyme-catalyzed amino-acid transfer reactions. *Nature* **381**, 442–444.

Lorsch, J.R. and Szostak, J.W. (1994) In vitro evolution of new ribozymes with polynucleotide kinase activity. *Nature* **371**, 31–36.

Lorsch, J.R. and Szostak, J.W. (1995) Kinetic and thermodynamic characterization of the reaction catalyzed by a polynucleotide kinase ribozyme. *Biochemistry* **33**, 15315–15327.

Luisi, P.L. (ed.) (2004) Prebiotic chemistry and early evolution. *Orig. Life Evol. Biosph.* **34**.

Luisi, P.L., Walde, P. and Oberholzer, T. (1994) Enzymatic RNA synthesis in self-reproducing vesicles: An approach to the construction of a minimal synthetic cell. *Ber. Bunsenges. Phys. Chem.* **98**, 1160–1165.

Marques, J.T., Devosse, T., Wang, D., Zamanian-Daryoush, M., Serbinowski, P., Hartmann, R. *et al.* (2006) A structural basis for discriminating between self and nonself double-stranded RNAs in mammalian cells. *Nat. Biotechnol.* **24**, 559–565.

Martinez, M.A., Vartanian, J.P. and Wain-Hobson, S. (1994) Hypermutagenesis of RNA using human immunodeficiency virus type 1 reverse transcriptase and biased dNTP concentrations. *Proc. Natl Acad. Sci. USA* **91**, 11787–11791.

Mason, S.F. (1991) *Chemical Evolution. Origin of the Elements, Molecules, and Living Systems.* Oxford: Clarendon Press.

Mattick, J.S. (2004) RNA regulation: A new genetics? *Nat. Rev.Genet.* **5**, 316–323.

Maynard Smith, J. and Szathmáry, E. (1995) *The Major Transitions in Evolution.* Oxford: W.H. Freeman.

McCaskill, J. (1984) A localization threshold for macromolecular quasispecies from continuously distributed replication rates. *J. Chem. Phys.* **80**, 5194–5202.

McCaskill, J.S. (1997) Spatially resolved in vitro molecular ecology. *Biophys. Chem.* **66**, 145–158.

McManus, M.T. and Sharp, P.A. (2002) Gene silencing in mammals by small interfering RNAS. *Nat. Rev.Genet.* **3**, 737–747.

Mills, D.R., Peterson, R.L. and Spiegelman, S. (1967) An extracellular Darwinian experiment with a self-duplicating nucleic acid molecule. *Proc. Natl Acad. Sci. USA* **58**, 217–224.

Moya, A., Elena, S.F., Brancho, A., Miralles, R. and Barrio, E. (2000) The evolution of RNA viruses: A population genetics view. *Proc. Natl Acad. Sci. USA*, **97**, 6967–6973.

Moya, A., Holmes, E.C. and González-Candelas, F. (2004) The population genetics and evolutionary epidemiology RNA viruses. *Nat. Rev. Microbiol.* **2**, 279–288.

Mullis, K.B. (1990) The unusual origin of the polymerase chain reaction. *Sci. Am.* **262**, 36–43.

Nicolis, G. and Prigogine, I. (1977) *Self-Organization in Nonequilibrium Systems. From Dissipative Structures to Order through Fluctuations.* New York: John Wiley & Sons.

Nissen, P., Hansen, J., Ban, N., Moore, P.B. and Steitz, T.A. (2000) The structural basis of ribosome activity in peptide bond synthesis. *Science* **289**, 920–930.

Noller, H.F., Hoffarth, V. and Zimniak, L. (1992) Unusual resistance of peptidyl transferase to protein extraction procedures. *Science* **256**, 1416–1419.

Nowak, M. and Schuster, P. (1989) Error thresholds of replication in finite populations. Mutation frequencies and the onset of Muller's ratchet. *J. Theor. Biol.* **137**, 375–395.

Nowick, J.S., Feng, Q., Ballester, T. and Rebek, J., Jr. (1991) Kinetic studies and modeling of a self-replicating system. *J. Am. Chem. Soc.* **113**, 8831–8839.

Orgel, L.E. (1986) RNA catalysis and the origin of life. *J. Theor. Biol.* **123**, 127–149.

Orgel, L.E. (1987) Evolution of the genetic apparatus. A review. *Cold Spring Harbor Symp. Quant. Biol.* **52**, 9–16.

Orgel, L.E. (1992) Molecular replication. *Nature* **358**, 203–209.

Orgel, L.E. (2003) Some consequences of the RNA world hypothesis. *Orig. Life Evol. Biosph.* **33**, 211–218.

Palsson, B.Ø. (2006) *Systems Biology. Properties of Reconstructed Networks.* New York: Cambridge University Press.

Pastor-Satorras, R. and Solé, R.V. (2001) Reaction-diffusion model of quasispecies dynamics. *Phys. Rev. E* **64**, 051909.

Pflug, H.D. and Jaeschke-Boyer, H. (1979) Combined structural and chemical analysis of 3.800-Myr-old microfossils. *Nature* **280**, 483–486.

Pley, H., Flaherty, K. and McKay, D. (1994) Three-dimensional structures of a hammerhead ribozyme. *Nature* **372**, 68–74.

Prudent, J.R., Uno, T. and Schultz, P.G. (1994) Expanding the scope of RNA catalysis. *Science* **264**, 1924–1927.

Rasmussen, S., Chen, L., Nilsson, M. and Abe, S. (2003) Bridging nonliving to living matter. *Artif. Life* **9**, 269–316.

Rasmussen, S., Chen, L., Stadler, B.M.R. and Stadler, P.F. (2004a) Proto-organism kinetics: Evolutionary dynamics of lipid aggregates with genes and metabolism. *Orig. Life Evol. Biosph.* **34**, 171–180.

Rasmussen, S., Chen, L., Deamer, D., Krakauer, D.C., Packard, N.H., Stadler, P.F. and Bedau, M.A. (2004b) Transitions from nonliving to living matter. *Science* **303**, 963–965.

Reidys, C.M. and Stadler, P.F. (2001) Neutrality in fitness landscapes. *Appl. Math. Comput.* **117**, 321–350.

Reidys, C.M., Stadler, P.F. and Schuster, P. (1997) Generic properties of combinatory maps: Neural networks of RNA secondary structures. *Bull. Math. Biol.* **59**, 339–397.

Reidys, C., Forst, C. and Schuster, P. (2001) Replication and mutation on neutral networks. *Bull. Math. Biol.* **63**, 57–94.

Saakian, D.B. and Hu, C.-K. (2006) Exact solution of the Eigen model with general fitness functions and degradation rates. *Proc. Natl Acad. Sci. USA*, **103**, 4935–4939.

Saakian, D.B., Muños, E., Hu, C.-K. and Deem, M.W. (2006) Quasispecies theory for multiple-peak fitness landscapes. *Phys. Rev. E* **73**, 041913.

Schidlowski, M. (1988) A 3.800-million-year isotope record of life from carbon in sedimentary rocks. *Nature* **333**, 313–318.

Schlögl, F. (1972) Chemical reaction models for non-equilibrium phase transitions. *Z. f. Physik A* **253**, 147–161.

Schopf, J.W. (1993) Microfossils of the early archean apex chert: New evidence of the antiquity of life. *Science* **260**, 640–646.

Schopf, J.W. (2006) Fossil evidence of Archaean life. *Philos. Trans. R. Soc. B*, **361**, 869–885.

Schuster, P. (1997a) Genotypes with phenotypes: Adventures in an RNA toy world. *Biophys. Chem.* **66**, 75–110.

Schuster, P. (1997b) Landscapes and molecular evolution. *Physica D* **107**, 351–365.

Schuster, P. (2003) Molecular insight into the evolution of phenotypes. In: *Evolutionary Dynamics—Exploring the Interplay of Accident, Selection, Neutrality, and Function* (J.P. Crutchfield and P. Schuster, eds), pp. 163–215. New York: Oxford University Press.

Schuster, P. (2006) Prediction of RNA secondary structures: From theory to models and real molecules. *Rep. Prog. Phys.* **69**, 1419–1477.

Schuster, P. and Sigmund, K. (1983) Replicator dynamics. *J. Theor. Biol.* **100**, 533–538.

Schuster, P. and Sigmund, K. (1985) Dynamics of evolutionary optimization. *Ber. Bunsenges. Phys.Chem.* **89**, 668–682.

Schuster, P. and Swetina, J. (1988) Stationary mutant distribution and evolutionary optimization. *Bull. Math. Biol.* **50**, 635–660.

Schuster, P., Fontana, W., Stadler, P.F. and Hofacker, I.L. (1994) From sequences to shapes and back: A case study in RNA secondary structures. *Proc. R. Soc. Lond. B* **255**, 279–284.

Schwartz, A.W. (1997) Speculation on the RNA precursor problem. *J. Theor. Biol.* **187**, 523–527.

Scott, W.G., Finch, J.T. and Klug, A. (1995) The crystal structure of an all-RNA hammerhead ribozyme: A proposed mechanism for RNA catalytic cleavage. *Cell* **81**, 991–1002.

Seelig, B. and Jäschke, A. (1999) A small catalytic RNA motif with Diels-Alder activity. *Chem. Biol.* **6**, 167–176.

Segel, L.A. and Slemrod, M. (1989) The quasi-steady state assumption: A case study in perturbation. *SIAM Rev.* **31**, 446–477.

Seneta, E. (1981) *Non-negative Matrices and Markov Chains*, 2nd edn. New York: Springer-Verlag.

Serganov, A., Keiper, S., Malinina, L., Terechko, V., Skripkin, E., Höbartner, C. *et al.* (2005) Structural basis for Diels-Alder ribozyme-catalyzed carbon-carbon bond formation. *Nat. Struct. Mol. Biol.* **12**, 218–224.

Severin, K., Lee, D.H., Granja, J.R., Martinez, J.A. and Ghadiri, M.R. (1997) Peptide self-replication via template directed ligation. *Chemistry* **3**, 1017–1024.

Soai, K., Shibata, T., Morioka, H. and Choji, K. (1995) Asymmetric autocatalysis and amplification of enantiomeric excess of a chiral molecule. *Nature* **378**, 767–768.

Spiegelman, S. (1971) An approach to the experimental analysis of precellular evolution. *Q. Rev. Biophys.* **4**, 213–253.

Stadler, B.M.R. and Stadler, P.F. (2003) Molecular replicator dynamics. *Adv. Complex Syst.* **6**, 47–77.

Stadler, B.M.R., Stadler, P.F. and Schuster, P. (2000) Dynamics of autocatalytic replicator networks based on higher order ligation reactions. *Bull. Math. Biol.* **62**, 1061–1086.

Stadler, P.F. (1991) Complementary replication. *Math. Biosci.* **107**, 83–109.

Stadler, P.F. and Stadler, B.M.R. (2007) Replicator dynamics in protocells. In: *Protocells: Bridging Nonliving and Living Matter* (S. Rasmussen, M. Bedau, L. Chen, D. Deamer, D.C. Krakauer, N.H. Packard and P.F. Stadler, eds) MIT Press. in press.

Steitz, T.A. and Moore, P.B. (2003) RNA, the first molecular catalyst: The ribosome is a ribozyme. *Trends Biochem. Sci.* **28**, 411–418.

Swetina, J. and Schuster, P. (1982) Self-replication with errors—A model for polynucleotide replication. *Biophys. Chem.* **16**, 329–345.

Szathmáry, E. and Gladkih, I. (1989) Sub-exponential growth and coexistence of non-enzymatically replicating templates. *J. Theor. Biol.* **138**, 55–58.

Szathmáry, E. and Maynard Smith, J. (1997) From replicators to reproducers: The first major transition leading to life. *J. Theor. Biol.* **187**, 555–571.

Takeuchi, N. and Hogeweg, P. (2007) Error-thresholds exist in fitness landscapes with lethal mutants. *BMC Evol. Biol.* **7**, 1–11.

Takeuchi, N., Poorthuis, P.H. and Hogeweg, P. (2005) Phenotypic error-threshold: Additivity and epistasis in RNA evolution. *BMC Evol. Biol.* **5**, 1–9.

Tannenbaum, E., Deeds, E.J. and Shakhnovich, E.I. (2004) Semiconservative replication in the quasispecies model. *Phys. Rev. E* **69**, 061916.

Tannenbaum, E., Shirley, J.L. and Shakhnovich, E.I. (2006) Semiconservative quasispecies equations for polysomic genomes: The haploid case. *J. Theor. Biol.* **241**, 791–805.

Tarazona, P. (1992) Error-tresholds for molecular quasispecies as phase transitions: From simple landscapes to spinglass models. *Phys. Rev. A* **45**, 6038–6050.

Thompson, C.J. and McBride, J.L. (1974) On Eigen's theory of the self-organization of matter and the evolution of biological macromolecules. *Math. Biosci.* **21**, 127–142.

Tjivikua, T., Ballester, P. and Rebek, J., Jr. (1990) A self-replicating system. *J. Am. Chem. Soc.* **112**, 1249–1250.

Tsukiji, S., Pattnaik, S.B. and Suga, H. (2004) Reduction of an aldehyde by a NADH/Zn^{2}+ -dependent redox active ribozyme. *J.Am.Chem. Soc.* **126**, 5044–5045.

Turing, A.M. (1952) A chemical basis of morphogenesis. *Philos. Trans. R. Soc. Lond. B* **337**, 37–72.

Uhlenbeck, O.C. (1987) A small catalytic oligoribonucleotide. *Nature* **328**, 596–600.

Valandro, L., Salvato, B., Caimmi, R. and Galzigna, L. (2000) Isomorphism of quasispecies and peroclation models. *J. Theor. Biol.* **202**, 187–194.

Varga, S. and Szathmáry, E. (1997) An extremum principle for parabolic competition. *Bull. Math. Biol.* **59**, 1145–1154.

von Kiedrowski, G. (1986) A self-replicating hexadeoxynucleotide. *Angew. Chem. Int. Ed. Engl.* **25**, 932–935.

von Kiedrowski, G. (1993) Minimal replicator theory I: Parabolic versus exponential growth. In: *Bioorganic Chemistry Frontiers*, Vol. 3, pp. 115–146. Berlin and Heidelberg: Springer-Verlag.

Wagner, G.P. and Krall, P. (1993) What is the difference between models of error thresholds and Muller's ratchet? *J. Math. Biol.* **32**, 33–44.

Watts, A. and Schwarz, G. (eds) (1997) Evolutionary Biotechnology—From Theory to Experiment. Special *Issue of Biophys. Chem.* **66**, 67–284.

Wecker, M., Smith, D. and Gold, L. (1996) In vitro selection of a novel catalytic RNA: Characterization of a sulfur alkylation reaction and interaction with a small peptide. *RNA* **2**, 982–994.

Weissmann, C. (1974) The making of a phage. *FEBS Lett.* (*Suppl.*) **40**, S10–sS12.

Wiehe, T. (1997) Model dependency of error thresholds: The role of fitness functions and contrasts between the finite and the infinite sites models. *Genet. Res. Camb.* **69**, 127–136.

Wilke, C.O. (2001) Selection for fitness versus selection for robustness in RNA secondary structure folding. *Evolution* **55**, 2412–2420.

Wilke, C.O. (2005) Quasispecies theory in the context of population genetics. *BMC Evol. Biol.* **5**, 1–8.

Wilke, C.O. and Ronnewinkel, C. (2001) Dynamic fitness lansdscapes: Expansions for small mutation rates. *Physica A* **290**, 475–490.

Wilke, C.O., Ronnewinkel, C. and Martinetz, T. (2001) Dynamic fitness lansdscapes in molecular evolution. *Phys. Rep.* **349**, 395–446.

Wills, P.R., Kauffman, S.A., Stadler, B.M. and Stadler, P.F. (1998) Selection dynamics in autocatalytic systems: Templates replicating through binary ligation. *Bull. Math. Biol.* **60**, 1073–1098.

Wilson, C. and Szostak, J.W. (1995) In vitro evolution of a self-alkylating ribozyme. *Nature* **374**, 777–782.

Wlotzka, B. and McCaskill, J.S. (1997) A molecular predator and its prey: Coupled isothermal amplification of nucleic acids. *Chem. Biol.* **4**, 25–33.

Wright, S. (1932). The roles of mutation, inbreeding, crossbreeeding and selection in evolution. In: D.F. Jones (ed.), *International Proceedings of the Sixth International Congress on Genetics*, Vol. 1, pp. 356–366.

Zhang, B. and Cech, T.R. (1997) Peptide bond formation by in vitro selected ribozymes. *Nature* **390**, 96–100.

Zhang, B. and Cech, T.R. (1998) Peptidyl-transferase ribozymes: Trans reactions, structural characterization and ribosomal RNA-like features. *Chem. Biol.* **5**, 539–553.

ORIGIN AND EVOLUTION OF VIRUSES

SECOND EDITION

Edited by

ESTEBAN DOMINGO
Centro de Biología Molecular "Severo Ochoa" (CSIC-UAM), Campus de Cantoblanco, 28049 Madrid, Spain
and CIBERehd

COLIN R. PARRISH
Cornell University, College of Veterinary Medicine, Baker Institute for Animal Health, Ithaca, NY 14853, USA

JOHN J. HOLLAND
Institute for Molecular Genetics and Division of Biology, University of California, San Diego, CA 92093, USA

ELSEVIER

AMSTERDAM • BOSTON • HEIDELBERG • LONDON
NEW YORK • OXFORD • PARIS • SAN DIEGO
SAN FRANCISCO • SINGAPORE • SYDNEY • TOKYO
Academic Press is an imprint of Elsevier

Academic Press is an imprint of Elsevier
32 Jamestown Road, London NW1 7BY, UK
30 Corporate Drive, Suite 400, Burlington, MA 01803, USA
525 B Street, Suite 1900, San Diego, CA 92101-4495, USA
360 Park Avenue South, New York, NY 10010-1710, USA

First edition 1999
Second edition 2008

British Library Cataloguing in Publication Data
A catalogue record for this book is available from the British Library

Library of Congress Cataloguing-in-Publication Data
A catalogue record for this book is available from the Library of Congress

ISBN: 978-0-12-374153-0

For information on all Elsevier publications
visit our web site at www.elsevierdirect.com

Typeset by Charon Tec Ltd., A Macmillan Company.
(www.macmillansolutions.com)

Printed and bounded in Hungary

08 09 10 11 12 10 9 8 7 6 5 4 3 2 1

Contents